

HIGH-RATE WIRELESS DATA COMMUNICATIONS: AN UNDERWATER ACOUSTIC COMMUNICATIONS FRAMEWORK AT THE PHYSICAL LAYER

ANTHONY G. BESSIOS* and FRANK M. CAIMI†*

*Department of Electrical Engineering, Harbor Branch Oceanographic Institution, Inc.,
5600 U.S. 1 North, Fort Pierce, FL 34946*

(Received 20 October 1995)

A variety of signal processing functions are performed by Underwater Acoustic Systems. These include: 1) detection to determine presence or absence of information signals in the presence of noise, or an attempt to describe which of a predetermined finite set of possible messages $\{m_i, i = 1, \dots, M\}$ the signal represents; 2) estimation of some parameter $\hat{\theta}$ associated with the received signal (i.e. range, depth, bearing angle, etc.); 3) classification and source identification; 4) dynamics tracking; 5) navigation (collision avoidance and terminal guidance); 6) countermeasures; and 7) communications. The focus of this paper is acoustic communications.

There is a global current need to develop reliable wireless digital communications for the underwater environment, with sufficient performance and efficiency to substitute for costly wired systems. One possible goal is a wireless system implementation that insures underwater terminal mobility. There is also a vital need to improve the performance of the existing systems in terms of data-rate, noise immunity, operational range, and power consumption, since, in practice, portable high-speed, long range, compact, low-power systems are desired.

We concede the difficulties associated with acoustic systems and concentrate on the development of robust data transmission methods anticipating the eventual need for real time or near real time video transmission. An overview of the various detection techniques and the general statistical digital communication problem is given based on a statistical decision theory framework. The theoretical formulation of the underwater acoustic data communications problem includes modeling of the stochastic channel to incorporate a variety of impairments and environmental uncertainties, and proposal of new compensation strategies for an efficient and robust receiver design.

1. INTRODUCTION

Any underwater acoustic communications system (ACS) approach must consider effects of the environment on error rates, range transmission speed, and system complexity. In the ocean, environmental parameters are non-stationary and exhibit geographic as well as variability with operational depth at each communication element or node. The success of any ACS therefore depends upon its ability to operate and possibly adapt to randomly variable conditions. These conditions include the formation of deep or shallow ocean acoustic ducts (waveguides) that exhibit modal behavior with corresponding multipath and reverberation interference. Modes can be supported over long distances in deep water, and can provide effective, but low data channel capacity, communications. As with any waveguide, the eigenfunctions and associated eigenvalues are determined by specific

*Corresponding author. Tel.: (407)465-2400, ext. 256 or (407)567-7196, Ext. 256.

Tl: 52-2886. Fax: (407)464-9094

*E-mail: agbe@msg.ti.com *†E-mail: caimi@hboi.edu

physical parameters, including in the underwater case, thermal (acoustic speed) profiles which affect wave refraction in the geometrical sense through Fermat's Law, acoustic frequency or wavenumber associated with the signals of interest, as well as location of perturbations to the waveguide physical structure either along or crosswise to the flow of energy. The air/water and water/substrate interfaces are highly reflective and can result in the formation of channels near the surface or at depth, and can create simple Fresnel reflections that contribute to reverberation of emitted signals over the transmit/receive path. This multimodal propagation is a common phenomenon over horizontal propagation paths, while reverberation between upper and lower boundaries is often a limitation even in vertical (surface to bottom) communications.

The response of the communications channel, (waveguide only) is not lossless, and is governed by frequency dependent absorption and scattering processes, as well as by the waveguide response for the excited modes. The absorption and scattering increase significantly with frequency ($\propto f^n$), thereby reducing the broadcast signal amplitude in relation to either ambient or detection-induced noise. Other factors, affecting underwater communications are path losses due to geometrical spreading (see Fig. 1), and Gaussian ambient noise, which decreases with frequency. Usually the ambient noise is encountered at low frequencies and is localized. In addition, there is the flow noise turbulent boundary which is a Gaussian random process having a power spectrum which is a function of speed, as well as Doppler spreading due to relative motion. The result is a limitation in usable bandwidth as the transmission distance is increased. This effect, combined with the frequency selective propagation occurring as a result of coherent addition among modes, establishes a relatively narrow bandwidth for transmission over a fixed communication distance, and can create deep frequency nulls that are environmentally dependent.

A description of the environmental parameters of the ocean and its associated waveguiding properties can be found elsewhere [95]. Generally, the entire channel is limited to relatively small frequency range (<1 MHz) in comparison to radio frequency channels, (extending well into the GHz region), but is characterized by many of the same measures, such as impulse response and coherence, where phase sensitive detection is required.

In order to allow more robust communications within the physical limitations of the underwater acoustic channel, it is customary to resort to either frequency or spatial diversity methods, as is common in low frequency communications. The implementation of equalization, i.e. the weighting and combination of multiply delayed channels within

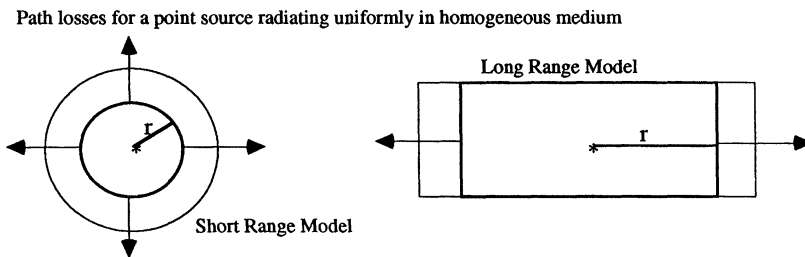


Figure 1 Free space spherical geometry $\sim 1/r^2$ (left) Cylindrical model horizontal stratified geometry $\sim 1/r$ (right).

the receiver prior to detection, is highly desirable and can extend the usable bandwidth and channel capacity of the system. In particular, a combination of diversity and adaptive equalization techniques can produce the most efficient use of the channel. Thus, we will focus on equalization methods that use advanced signal processing techniques to achieve the high data rates characteristic of video, and other high speed data transmissions. The propagation conditions of the oceanic channel set the specifications for the model design that we propose.

In this paper, we consider the effect of *reverberation* due to multipath, which creates a colored non-flat spectrum. To equalize a system with this kind of non-white input, it is necessary to rely upon a-priori information regarding the correlation properties of the colored received data (i.e. a 2nd-order statistics model $\in \{S^{(2)}\}$). The induced optimization problem creates a nonlinear function in terms of the equalizer output z_n derived in section IV.A.

This paper is current in that a significant amount of research has been conducted in the general subject area over the past several years [1–101]. For instance, various novel methods have been developed and employed for data transmission over different types of media with substantial improvements in performance being noted [4], [19], [35], [39], [40], [46], [52], [57–58], [61], [63], [65], [81], [87], [89], [98–99], and [101–103]. Particular progress has been made in the development of video compression techniques for wireless communications [4], [52], [57], [63], [87], and [101], beamforming [21], [24], [32–33], [41], [61], [66], [76], and [104] and equalization [6], [8], [12–14], [31], [37–38], [43], [47], [59], [64], [67], [71–72], [78], [83–86], [90], [94], and [102–103] (conventional equalization technology) for wired and wireless (tropospheric digital radio) high-speed communication links via bandlimited channels subject to Intersymbol Interference (ISI) and additive noise. Multipath and frequency-selectivity consist a common type of distortion for wireless communication environment. Research on behalf of other investigators [10–11], [16–17], [22–23], [26–29], [45], [51], [54–55], [77], [84], and [100] has greatly improved the ability to conduct acoustic data communications in the ocean channel through the use of improved data modulation methodologies and advanced signal processing techniques.

There are relatively few studies however, that address the problem associated with **self-adaptive (blind)** equalization alone, or compound strategies of blind equalization with spatial/frequency **diversity** reception schemes. The blind/self adaptive scheme is able to obtain equalizer tap-adjustment without having access to the transmitted data except of some a-priori statistics, and is the proper architectural structure for Point-to-Multipoint (P-MP), Multichannel Multipoint Distribution Service (MMDS) Acoustic Systems (see section III.D). The *supplementarity* of equalization and spatial diversity reception has also well been established in underwater acoustics and digital radio communications. On the other hand, there are various contributions regarding the *complementarity* of equalization and beamforming [45]. For vertical transmission or deep ocean channels the multipath is sufficiently canceled by beam steering alone. As the range increases the array becomes gradually unable to resolve single propagation paths, and the need for equalization arises. Increasing the directivity index and concentrating the power of the transmitted beam can also provide additional performance improvement. With sufficient directivity, an approximation to a Line-of-Sight (LOS) system is achieved. Gain and noise reduction on the order of 10–30 dB are achievable by placing nulls on the planar interference direction, but pointing errors can be a complicating issue. Depending on the degree of mobility, systems

may be classified as mobile and semimobile, with a need for omnidirectional and partially or highly directive transducers respectively. The directivity can be relaxed as the system requirements are relaxed from nonstationary to relatively more stationary application environments.

Further exploitation of unique propagational properties of the ocean [51] leads to the proposal of a **multicarrier modulation scheme (MCM)**, whereby interleaved bit streams modulate more than one carrier to enhance usage of available bandwidth, improving the Bit-Error-Rate (BER) performance, and consequently reduce the need for equalization at the receiver. Since MCM may be considered a predistortion, or equivalently as an equalization technique applied at the transmitter, it is effective for reduction of the hardware complexity at the receiver. Many of the concepts developed for the optimization of underwater communication system performance are inherently nonlinear in nature and are suitably described in this paper.

2. PRELIMINARIES

A. Statistical Decision Theory for Data Communications

A statistical decision theory framework for general digital communications applications could be briefly described as follows (see Fig. 2):

- The signal parameter space $\mathcal{Q} \subset \mathbf{C}$, or \mathbf{R} (subset of the set of complex or real numbers respectively) of operating points q , or under a statistical framework, the state of nature q (statistical models of signal and noise spectra, with prior probability density functions (pdf's) $\pi(q)$),
- The space \mathcal{A} of strategies, or decision rules, or actions α (filters, detectors, estimators) forming randomized or nonrandomized decision rules,
- The space \mathcal{G} with observations $y^{(s)}$, and
- The space \mathcal{M} of performance measures (Mean Squared Error MSE, Signal-to-Noise Ratio SNR, Probability of Error P_e).

The communication channel, independent of the medium type, can be seen as the conditional pdf, that statistically characterizes the channel, and is mapping from signal

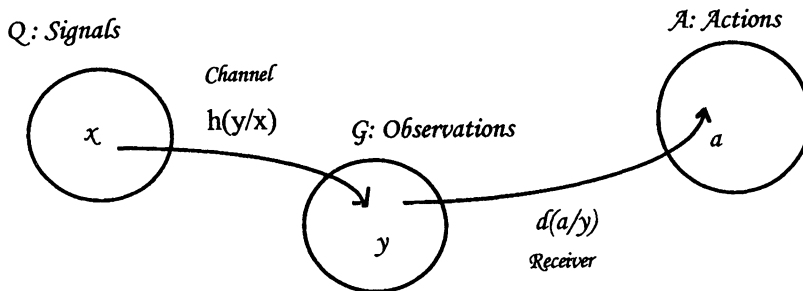


Figure 2 The statistical communication model.

space $\mathcal{Q} \xrightarrow{\text{into}} \mathcal{G}$ observation space. The receiver can be seen as a mapping from the observation space $\mathcal{G} \xrightarrow{\text{into}} \mathcal{A}$ the decision space. Optimal receiver design is accomplished by determining a deterministic or probabilistic map based on some designated criterion.

Analysis of decision problems in terms of utility functions $U(r)$, where r represents the reward determined by the pair of the operating points designated by q and the corresponding action α , can conclude with the formulation of squared error loss $MSE L(q, \alpha) = (q - \alpha)^2$, absolute error loss $L(q, \alpha) = |q - \alpha|$, weighed linear error loss, 0-1 loss (binary hypothesis), uniform cost function, etc. (see Fig. 11). If the performance criterion is an even, non- decreasing function of $|q - \alpha|$, and the a-posteriori probability density function (pdf) $\pi^*(q/y)$ (i.e., the data modified version of the a-priori pdf $\pi(q)$, after observation of the data y_n) is unimodal and symmetric, then the optimum action or estimator α is the conditional mean: $\alpha = E(q/y)$. The loss functions are determined based on knowledge of the possible consequences of the decision. Decision making in the presence of uncertainty leads to expected types of losses ; for instance, the concept of robustness or uncertainty tolerance in an inferential framework is presented in [74] with emphasis on the game theoretic formulation of minimax robustness. The solution can be very conservative under a minimax robust procedure but the assumption of a set of small perturbations alleviates any risk associated with large minimax range. The minimax approach may lead to bad decision rules, however it is suitable when no prior information is available, and it protects against the worst possible {state of nature} q . Saddlepoints or least favorable operating points are the objective by optimizing concave-convex cost functions: $\inf_{\alpha \in \mathcal{A}} \sup_{q \in \mathcal{Q}} M(\alpha, q)$.

A top-down approach for the digital communications receiver design problem would follow the following set of actions:

- 1) Formulate communications as a binary/M-ary hypothesis testing problem from the decision theory,
- 2) Design coherent communications with scalar signals, and coherent communications with vector signals (binary/M-ary) over the discrete memoryless channel,
- 3) Then design coherent communications with waveforms over the continuous memoryless channel. The Additive White Gaussian Noise (AWGN) channel assumption provides linear detectors i.e. linear functions of the received signal, however in the general case of a channel with an arbitrary pdf the detection process becomes a *nonlinear* problem.

Matched filtering (where the objective is maximization of the output SNR level using linear time invariant (LTI) filter) is designed to be tolerant to uncertainty in the second-order spatial or temporal correlation structure of signals (information and noise). The derivation of the matched filter is based on the Schwartz inequality:

$$\frac{|\int f(t)g(t)dt|^2}{\int |f(t)|^2 dt \int |g(t)|^2 dt} \leq 1, \text{ with equality iff } f(t) = kg^*(t) \tag{1}$$

by setting $f(t) = h(t)$, and $g(t) = x(t_0 - t)$ the matched filter will be given by (see fig. 3):

$$h(t) = kx^*(t_0 - t) \leftrightarrow H(f) = kX^*(f)e^{-j2\pi ft_0} \Rightarrow \max SNR \tag{2}$$

Various optimum receivers have been developed under the framework of vector communications over a memoryless channel. Those receivers emanate from Statistical Decision Theory (e.g., the binary/M-ary hypothesis testing problem), such as [9], [96]: Bayes, Neyman-Pearson, Probability-of-Error (P_e), maximum-a-posteriori (MAP) using the posterior pdf $\pi^*(q/x)$ (see Fig. 4), Maximum Likelihood (ML) for the special case that the a-priori probabilities are equal, and minimum distance decoding under the assumptions of equally probable messages and the Additive White Gaussian Noise (AWGN) channel (see fig. 5). Note that there are techniques using the so-called “non-informative priors” that can provide MAP receivers when prior data information is not available [9]. Bayesian analysis is the statistical approach which formally seeks to utilize prior information. The M-ary hypothesis problem can be formed as follows:

$$\begin{aligned} & \left\{ \begin{array}{c} \text{Hypothesis} \\ \updownarrow 1-i_0-1 \\ \text{Messages} \end{array} \right\} \\ \Rightarrow & \left\{ \begin{array}{ccc} H_0 & H_1 & H_{M-1} \\ \updownarrow: y = x_0 + n, & \updownarrow: y = x_1 + n, \cdot \cdot \cdot, & \updownarrow: y = x_{M-1} + n \\ m_0 & m_1 & m_{M-1} \end{array} \right\}, \\ & y \in \mathcal{G}, \quad x, n \in \mathcal{Q} \end{aligned}$$

For the special case where $M = 2$, and $x_0 = 0$ we have a description of the sonar/radar detection problem (binary hypothesis) where the presence or absence of an information signal needs to be determined.

A Neyman-Pearson formulation defines the following significant probabilities: $P_{FA} = P\{\text{dec } H_1/H_0 \text{ true}\}$ to provide a measure of the false alarm outcome and its waste of resources from which a cost function can be assigned, $P_{MISS} = P\{\text{dec } H_0/H_1 \text{ true}\}$ the miss is a catastrophic outcome and a cost function is not meaningful, $P_D = P\{\text{dec } H_1/H_1 \text{ true}\}$, $P_{CP} = P\{\text{dec } H_0/H_0 \text{ true}\}$. Hence, the design philosophy is to accept the largest number of false alarms that one could afford, and then find the posterior or conditional

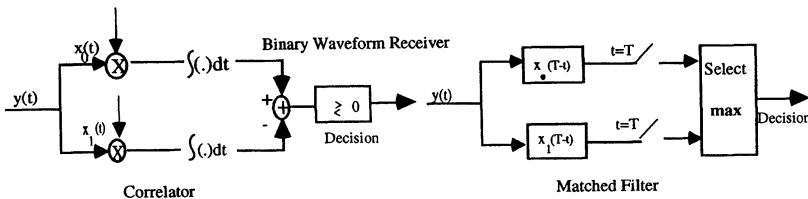


Figure 3 Equivalence between Correlator and Matched Filter Receiver.

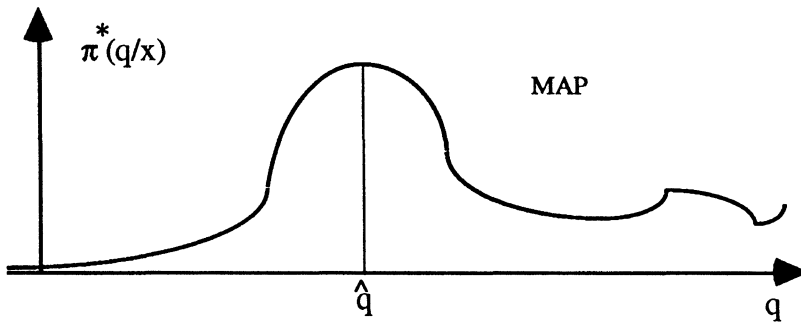


Figure 4 A hypothetical a-posteriori density.

decision rule $\delta(\alpha/y) \in \mathcal{A}$ to minimize the resulting probability of a catastrophe. The most important performance measure in these cases, is the Receiver Operating Characteristic (ROC) that provides the relationship: $P_D = f(P_{FA})$.

Adaptive equalizers follow the logic of the statistical sequential analysis [9]. The overall loss $L(q,\alpha,n,s)$ is considered to be the sum of the decision loss $L(q,\alpha)$ and an additional cost due to observation/sampling $C(n,s)$: $L(q,\alpha,n,s) = L(q,\alpha) + C(n,s)$ where n,s stand for the number of iterations (sample size), and the sampling methods respectively. To lower the value of the decision loss term, larger training data should be transmitted. Hence, in a sequential analysis mode, the observations are taken one at a time, with a decision made at each iteration, to either cease sampling and proceed with an action α , or otherwise assign in space \mathcal{A} an additional action α^* for taking another observation. A feedback link to the transmitter is necessary to tell it when to stop sending. So adaptive schemes based on a sequential type of statistical analysis allow one to gather exactly the correct amount of data needed for a decision of the desired accuracy. A sequential decision procedure can be notated as $d = (\tau,\delta)$ where τ,δ are the *stopping* and the *decision* rules respectively.

In systems driven by unobservable inputs, it is often desirable to recover attenuations and phase shifts of the transmitted data, or equivalently, to estimate the unknown channel impulse response. With the use of pilot signals, or with information derived after a preprocessing with a matched filter at the receiver, an estimate of attenuation and

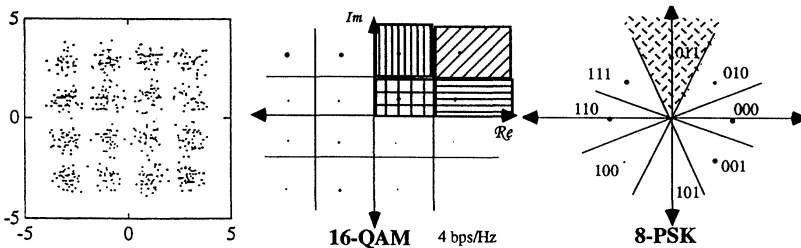


Figure 5 Accumulation over time of noise and ISI-perturbed received 16-QAM constellations (left)-Decision regions for ML detector (middle, right).

phase-shift of the transmitted signal can be obtained. It is evident from eq. (2) that the matched filter assumes an exactly known present signal, white noise, and a LTI filter, however, it does not depend on the waveform shape. A common characteristic for the aforementioned receivers is the requirement for a-priori knowledge of the transmitted signature sequences, prior data pdf's $\pi(q)$, or channel state information, i.e., some a-priori description of the communication channel impulse response. Therefore, conventional adaptive equalizers, e.g., based on Least Mean Square (LMS), and Recursive Least Squares (RLS) adaptive algorithms [35], [42], would require transmissions of previously known training sequences to the receiver. This wasteful process can be avoided by utilizing a *blind-type receiver* formulation [35], [43], which only requires some statistical information about the transmitted data and can obtain equalization/identification directly from the received distorted data (some partial statistical information regarding the originally transmitted data may also be necessary). It has been well established that it is the introduction of some type of *nonlinearity* that can allow accurate phase information recovery [43]. The desired nonlinearity can be introduced either at the input (Higher-order statistics-based) or the output (Bussgang-type) of the equalizer, or it can be embedded within the structure of the data detection process (probabilistic; Maximum Likelihood Sequence Estimation MLSE-type).

B. Sonar vs Radar

In this section we summarize the differences encountered in the radar, and sonar propagation environments. In sonar the speed of propagation of the sound is comparable to that of the target, causing Doppler shifts (0.7 Hz/KHz/Kt) significant enough to produce concerns about platform motion. For radars the Doppler shift is of the order of 3.4 Hz/GHz/Kt. Passive detection is a major sonar mode that does not exist in radar. However, there are various passive detection methods used in radio frequency jamming and target identification applications. No polarization concept exists in undersea acoustics. The ocean is very inhomogeneous and non-stationary, causing multipath, non-constant speed of propagation, and shadow zones. Sonars operate at the lower frequency bands (\sim KHz) for long range applications and up to 500 KHz for short range applications. Radars typically operate at the S-Band (near 3 GHz), but range from the UHF region (400 MHz) into the millimeter wave portion of the spectrum (100–500 GHz). Passive sonar is often broadband while conventional radar is usually narrowband. The ratio of propagation velocities is of the order 2×10^5 . The time delay for a 2-way travel (2,000 yds) for a sonar is 2.4 sec, and for the radar is 12.2 μ sec. The attenuation is much higher for sonars (2 dB/Kyd at 15 KHz) than in radars 0.02 dB/Kyd at 3 GHz. The ambient noise in the underwater environment is 60 dB higher than the cosmic noise, and the flow noise is 30 dB higher than the ambient. The propagation in sonar follows many paths, while in radar it is LOS.

Conclusively, the underwater acoustic propagation environment is a very noisy, highly attenuating, multipath fading environment with significant Doppler shifts, large number of interference sources, and virtually nonexistent support of pulse-to-pulse correlation. Hence, signal processing techniques specifically for the problems arising in the singular oceanic environment are unique.

C. Digital Microwave Radio vs Underwater Acoustics Communications

In the different application area of the high-speed tropospheric microwave digital radio communication systems, operating at the 300 MHz–30 GHz band, analogous degradation phenomena (to the low data rate underwater acoustic communication systems) are observed. In microwave systems reliable data rates are desired at 100s Mb/s using modulation schemes of high spectral efficiency such as 16-QAM or 64-QAM for optimum use of the available bandwidth. A high level of amplitude states in the transmitted signal constellation is necessary for high-capacity systems to efficiently utilize the limited available *radio* or *acoustic* spectrum. Also in microwave communications, the available spectrum is limited due to the very high demand by the large number of users, while in the latter case (although the demand is not large yet), bandwidth limitations exist due to increasing high frequency absorption and attenuation. However, the sensitivity of a digital radio or a digital acoustic system to all types of distortion increases with the number of points in the signal constellation, especially where the ISI effects start appearing.

The use of a frequency-selective channel structure may result in a common and unavoidable type of distortion/fading for wireless communication due to the multipath varying environment within the operating channel. Nevertheless, backscattering, ambient and flow noise, path losses, and Doppler spreads due to relative motion, are additional impairments encountered in the underwater acoustics that uniquely characterize the communication environment. The multipath propagation problem and its induced degradation effects such as ISI, have been encountered in many application fields: indoor, outdoor, and rural wireless terrestrial digital communications, tropospheric microwave digital radio links (troposcatter channel), etc.. The channel coherence bandwidth $(\Delta f)_c$ in the case of indoor communications (large offices and rooms) is in the range of 2–5 MHz; for smaller rooms $(\Delta f)_c > 10$ MHz; and for rural communications the multipath spread T_M is of the order $\sim 1\mu$ sec with a corresponding coherence bandwidth $(\Delta f)_c \sim 1$ MHz (see Table I).

Similar effects appear in the underwater acoustic environment where the multipath spreads are orders of magnitude higher implying a reduced channel coherence bandwidth which results in a system performance capable of accommodating only lower bit rates. Hence, in underwater applications the transmission parameters, rates, and environmental conditions differ significantly. The multipath spread T_M in the underwater channel can vary from 50 ms up to the order of several seconds depending upon the application and associated range. For shallow-water, long-range communications (up to several km) $T_M \sim 1$ –3 sec, and the Doppler spread B_D may be of the order of several Hz (see Table I). The longer the communication range the higher the multipath spread due to increased delays and number of multipath arrivals. The available bandwidth W is of the order of several 100s KHz for practical short, and/or long range applications. The following basic result derived by Shannon, regarding the capacity C of a bandlimited channel, provides a lower bound for the required transmission signal power P_s :

$$C = \underset{\sim \text{several hundreds KHz}}{W} \log_2 \left(1 + \frac{P_s}{WN_0} \right) \text{ bits/sec}$$

TABLE I Channel Coherence BW, Multipath & Doppler Spread for Multipath Time-variant Channels

	Channel Coherence (Δf) _C	Multipath Spread T_M	Doppler Spread B_D	Spread Factor $T_M B_D$
1. Troposcatter Channel SHF	1 MHz	~1 μ sec	0.1–10 Hz	10^{-5} underspread
2. Ionospheric HF/VHF	100 Hz–10 KHz	100 μ sec–10 msec	0.1–100 Hz	10^{-4} – 1 underspread
3. Outdoor	Rural terrestrial dig.: ~1 MHz	~1 μ sec	—	underspread
4. Indoor	Large offices and rooms: ~2–5 MHz Smaller rooms: >10 MHz	0.2–0.5 μ sec <0.1 μ sec	—	underspread
5. Underwater Acoustics	0.3 Hz–several kHz	0.3 ms–3sec	3–60 Hz	underspread & overspread

Thus, the underwater channel consists of a difficult medium to achieve high bit rates, leading to a definition of “very high speed transmission” that is at substantially lower rates as compared to radio-based systems. In this environment, a failure to meet temporal/frequential channel coherence constraints is common.

D. Modulation Issues for a High-Speed Underwater Modem

In the following we classify the priorities of the most critical criteria in the 4-dimensional design space of a modem for underwater operation, comprising:

1. Bandwidth efficiency,
2. Power efficiency,
3. Receiver complexity, and
4. Immunity to nonlinearities.

We treat various modulation methods, which are adequately defined and described in detail elsewhere [35].

1) Single-Carrier Modulation (SCM)—Underspread Channels

The optimal signal sets $\{x_i \in \mathcal{Q}, i = 1, \dots, M\}$ lie in the class of linearly dependent sets of vectors since they present a greater $P_D, \forall SNR$ than their corresponding independent ones $\{x_i \in \mathcal{Q}, i = 1, \dots, M\}$. Furthermore, in 2-dimensions the optimal signal set that obtains $\max P_D, \forall SNR$ consists of the M signal vectors equally spaced around the unit circle $\{x_i = e^{j2\pi i/M}, i = 1, \dots, M\}$ (see Figure 5). The signal constellations depending on the modulation type can be a subset of the set of real \mathbf{R} , or complex \mathbf{C} numbers. Noncoherent (FSK-type) detectors are simple in implementational sense, but they obtain poorer performance (e.g., for $M = 16, \gamma_b = SNR/bit = 8dB \rightarrow 10^{-5} < P_b^{(nonoch)} < P_b^{(coh)} = 10^{-6}$) and low bandwidth efficiency (1/2 of the corresponding M -ary orthogonal coherent bandwidth efficiency) in comparison to coherent methods of detection (PSK, QAM-type $\subset \mathbf{C}$).

Performance of the constellation against noise, is determined by the minimum distance between the signal points, e.g., $d_{\min}^{(16-QAM)} < d_{\min}^{(16-PSK)}$ (the spectral efficiency $\left(n \sim \log_2 \frac{2^n}{\# \text{ of signal points}} \right)$ of a 16-point constellation is ~ 4 bps/Hz, while of a 2-point is ~ 1 bps/Hz). However, the coherent detector's performance is degraded in the presence of multipaths and doppler shifts that exist in water nonstationary environmental conditions, so that smaller constellations may be preferred. Addition of differential detection can overcome the above difficulty with some loss in performance (~ 2.3 dB for QPSK, DQPSK at large $\gamma_b = SNR/bit > 10$ dB). In addition DPSK reduces the circuit implementation complexity (does not require intricate method for carrier phase estimation). Large QAM signal constellations (16-, 64-QAM) with signal points distributed uniformly in the complex plane, obtain an extremely high bandwidth efficiency, but they suffer in terms of power efficiency as compared with lower duty cycle methods. QPSK is a minimum-error constellation for Gaussian noise and shows best bandwidth efficiency, moderate immunity to nonlinearities and complexity. MSK is not recommended due to its poor bandwidth efficiency, and high implementation complexity. However, in parallel transmission schemes via frequency division multiplexed channels (see next section II.D.2), MSK presents lower *crossstalk* than QPSK if the guardband is > 0.7 bit rate of the individual channel [35]. Finally, MFSK is not preferred due to its poor bandwidth efficiency.

Channel coding has been successfully combined in satellite communications to compensate for power losses without sacrificing bandwidth efficiency. Constant Phase Modulation (CPM)-type modulations are coded modulations themselves. In general CPM shows an extraordinary joint power and bandwidth efficiency, at the expense of a higher hardware complexity. The reduced level of sidelobe energy in their spectra provides an additional advantage of system resistance to crosstalk effects. This method has yet to be tested for the underwater acoustic modem design, but would provide advantages for shallow water applications where intense multipath effects predominate.

SCM is sufficient when dealing with frequency-selective, fading channels, and the resulting system is underspread, i.e., $B_D T_M < 1$, where T_M is limited to a couple of symbols (the length of the equalizer N can be relatively short) and B_D is also sufficiently small to guarantee coherent processing of all transmitted symbols. In general the ocean acoustic channel is highly dispersive in time, but not in frequency. However, when a channel is characterized overspread, i.e., $B_D T_M > 1$ any waveform becomes severely distorted by induced ISI, implying that a serial transmission mode is inadequate. In this case, parallel schemes can prove to be adequate for achieving a desired degree of efficacy as discussed below.

2) Multicarrier Modulation (MCM)—Overspread Channels (see also section IV)

A novel approach to ACS design originates from the following significant observation about the sound propagation properties of the ocean. The surface duct and the deep sound

channel are two disjoint propagation paths with different transfer functions $H_S(\omega_1)$, $H_D(\omega_2)$ and optimum operational frequencies (see Figure 9). The energy leakage among the two ducts may be considered negligible and can be exploited judiciously through an MCM transmission scheme that encodes data over two subcarriers. It allows operation at multiples of the single-carrier transmission rate, by performing a data volume split over the multiple carrier modes. The system's immunity to distortions is increased due to incorporation of symbol guard space, while the equalizer's complexity at the reception point is relaxed. This design philosophy is characterized as an "equalization complexity split" between receiver and transmitter. More specifically, the longer the guard period the less the sensitivity to the multipath spread T_M . However, there is a trade-off between the BER and the guard period, since the longer the guard period the larger the inefficiency in terms of power and bandwidth. Each carrier operates at low data rate to reduce the probability of frequency selective fades destroying the data integrity, while the overall system performance is that of a high data rate system. MCM is inherently more robust to time-domain impulsive noise (e.g., biological generated impulsive noises, ice-cracking, etc.) due to the block processing nature in the frequency domain. MCM can deal with more severely overspread channels where serial-type transmission is inadequate. An MCM system has a higher error threshold than the single carrier modulation (SCM) scheme, and thus is inherently more immune even to impulsive-type impairments. There exists a dual reasoning behind the obtained receiver's complexity reduction:

- A complexity split between the transmitter and the receiver is accomplished, by performing joint equalization at both ends.
- Equalization of a narrowband subchannel requires equalizers of lower complexity, than that of wideband channel, and reduces the adverse effects of linear equalization; for example, additive noise enhancement. We consider the subchannel case where the signal becomes,

$$x(t) = \sum_{i=-\infty}^{\infty} \sum_{k=0}^1 \operatorname{Re} \{ \alpha_{ki} e^{j\omega_k(t-iT_S)} \} p(t - iT_S) \quad (4)$$

where $p(t)$ is the symbol pulse waveform $p(t) = \begin{cases} 1 & -\Delta \leq t \leq t_S \\ 0 & \text{otherwise} \end{cases}$

t_S is the observation period, α_{ki} are mutually independent i.i.d. data sequences, Δ is the guard space length, $T_S = \Delta + t_S$ is the extended symbol period, and $\omega_k = \omega_0 + 2\pi k / t_S$. The received waveform is then given:

$$y(t) = \int x(t - \tau)h(\tau;t)d\tau + n(t) \rightarrow y_{mi} = \frac{1}{t_S} \int_{iT_S}^{t_S+iT_S} y(t)e^{-j\omega_m(t-iT_S)} dt \quad (5)$$

For a time non-selective channel, it is assumed that the channel fluctuation can be neglected during a single transmission or even a few symbols, i.e., $T_S \ll 1/f_D$. MCM is inherently more robust to time-domain impulsive noise (e.g., biological generated impulsive noises) due to the block processing nature in the frequency domain.

Performance analysis of the MCM system can be derived [96] after determining the type of pdf $D_{mi}(\rho)$ that the random decision variable D_{mi} follows:

$$D_{mi} = R [y_{mi}y_{m(i-1)}^* e^{j\left(\frac{\pi}{2} - \frac{\pi}{M}\right)}] \tag{6}$$

The BER performance for MCM can be calculated based on the region that the decision variable D_{mi} takes value less than zero, thus, given distribution function of the decision variable $P(D_{mi} \leq x)$ we obtain P_e , as follows:

$$F_{D_{mi}}(x) = P(D_{mi} \leq x) = \int_{-\infty}^x D_{mi}(\rho) d\rho \Rightarrow P_e = F_{D_{mi}}(0) \tag{7}$$

It has been shown [39] that the BER $\in \mathcal{M}$ performance for frequency-selective fading channel is a function of the correlation coefficient $R_y(i)$ between consecutive received symbols of the same carrier: $R_y(i) = E\{y_{mi}y_{m(i-1)}^*\}/E\{y_{mi}y_{mi}^*\}$. The higher the correlation degree, the smaller the probability of error P_e :

$$P_e = P(D_{mi} < 0) = \int_{-\infty}^0 D_{mi}(x) dx = f(R_y(i)) \tag{8}$$

3. PROBLEM DEFINITION

A. Shallow vs Deep Water

In a non-dispersive channel free-space environment, the received signal would be only attenuated and delayed, but undistorted. Communicating in the ocean waveguide, an inhomogeneous dispersive medium with a Green's function $G(\omega, r)$ dependent on frequency, and at the reverberation-limited range where the noise-masking level of all other types of noises (ambient, flow, etc.) is lower than the reverberation level at the reception point, results in severely distorted signals (see fig. 6). A system description including the transfer function H or Green's function G is given in Section III.B. Wideband signals in the ocean are subject to both intermodal and intramodal-types of dispersion. The intermodal interference (IMI) among modes that travel along separated ducts (cochannel interference) is assumed negligible. However, this is not true for the IMI among modes traveling along the same duct and for ranges up to 40 km [97]. The intramodal dispersion appears at longer ranges in its most severe form, i.e. the ISI. For the ocean acoustic waveguide, an optimum multimode receiver would ensure coherent summation of the signals of each mode. Such compensation is highly desirable in shallow water horizontal channels described below. Another notable distortion, the reverberation, is a signal-dependent effect, so that properly designed transmitted waveform pulses, and receiver are required. When the source emits pulses short enough, and the receivers are

placed at sufficiently long range, then the travel times along the various paths, and the corresponding modes, become distinct so that multipath and time-dispersion can be treated separately [44]. This leads to the consideration of the depth and length of the channel. The Underwater Acoustic Communications can be classified as:

- *Shallow Water*: where depth is of the order of low-frequency wavelength,
- *Deep Water*: where depth is greater than low-frequency wavelength.

In Table II, it is provided a possible classification of the high frequency ocean acoustic data channels in terms of the communication range. Depending on the application, special design considerations are taken due to physical environmental constraints. The most difficult case is shallow water where multipath, reverberation, absorption, and bandwidth limitations are worst case.

For linear active systems the reverberation, (highly nonstationary), dominates mainly in the *shallow areas* with high range to depth ratios, or in the so-called *horizontal transmission mode*. It varies in space and time and it can be considered as a random time-varying linear function of the transmitted wave. In this regime, an increase of the transmitted power does not necessarily improve performance, and on the contrary, reducing power may have unexpectedly positive results since the reverberation is directly proportional to the energy in the transmission. The received spectra are usually Doppler-shifted and broader than the transmitted spectra mainly due to the relative motion, and the surface reverberation (multidirectional scattering of the surface reflected signal), as opposed to bottom reflections or volume scattering by fish, various suspended particulate and thermal or chemical variability. The reverberant environment causes both time and frequency spreading. The induced colored non-flat spectrum imposes certain conditions upon the equalization portion of the receiver design.

TABLE II Acoustic Data Channel Classification

	<i>Short-range</i> <i><1 km</i>	<i>Medium-range</i> <i>1–20 km</i>	<i>Long-range</i> <i>20–2000 km</i>
1. <i>Operational (carrier) Frequency</i>	10–50 kHz	~10 kHz	<10 kHz
2. <i>Transmitted Data pdf</i>	Non-Gaussian white i.i.d.	Non-Gaussian white i.i.d.	Non-Gaussian white i.i.d.
<i>Modulation</i>	MFSK, PSK	Non-coherent FSK Coherent	Phase—coherent
3. <i>Doppler Spread B_D</i> <i>Multipath Spread T_M</i>	10–60 Hz (17.5 Hz/kn) 2–22 msec (shallow)	50 Hz 50 ms – 1 sec	~mHz (no motion) 100's ms–3 sec shallow–deep
4. <i>Ambient Noise</i>	Gaussian	—	Non-Gaussian
5. <i>Equalization Type</i>	Linear, MAP, MLSE	Linear Adaptive	DFE
6. <i>Trasmission Type (depth)</i>	Horizontal (shallow)/Vertical (deep)	Horizontal	Horizontal
7. <i>Trasmission Speed</i>	Horizontal ~ 1.2 kbps Vertical > 20 kbps	—	—

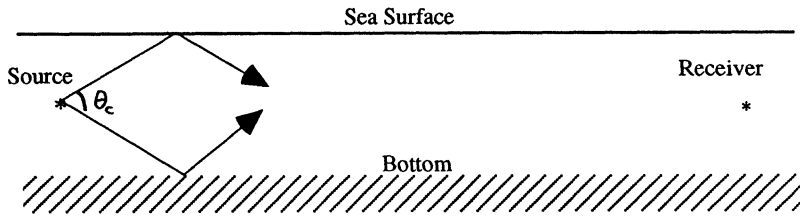


Figure 6 Waveguide model for sound propagation in shallow water within an aperture of $\theta_c = \frac{\theta_c}{2}$ (the critical angle).

B. The Multisensor Model

Vector communications serve as the platform for the more practical problem formulation of waveform coherent communications, where matched filter and correlator receiver implementations can be employed, but would require knowledge of the transmitted signature sequences. The bandlimited continuous waveform $x(t):[-W, W]$ communication problem can be faced in terms of discrete vector communication theory by sampling the continuous waveform at the proper rate $\Delta t = 1 / 2W$, and forming a vector of uncorrelated timesamples: $\bar{x}^T = [x(\Delta t), x(2\Delta t), \dots, x(M\Delta t)]$, $\bar{N}^T = [n(\Delta t), n(2\Delta t), \dots, n(M\Delta t)]$, $M = 2TW$ independent samples for $[0, T]$.

An efficient way to deal with the randomly varying reliability of the multipath channels, would be to introduce redundancy on the information-bearing signal. Then the transmission would take place in a multichannel digital signaling mode; i.e. the same information-bearing signal traversing physically disjoint paths, to overcome the unreliable channel of the group subject to short fades. In spatial multichannel digital signaling, the frequency selective, slowly fading channels are modeled by tapped delay lines with statistically independent, time-variant tap weights. A spatial diversity structure is implied for the vertical receive array consisting of two or more well separated sensors. Provided the spacing of the sensors is adequate to control their spatial coherency (\sim several wavelengths), a desired independence of the multiple measurements is achieved. Channel filters with transfer functions \bar{H}_n are considered, which can be expressed by some parametric model: Moving Average (MA), Autoregressive (AR), or Autoregressive-Moving Average (ARMA). In the case of a system with *only zeros* inside and outside of the unit circle (non-minimum-phase systems MA, or Finite Impulse Response FIR) the system is sufficiently described by its impulse response \bar{h}_n .

$$H^{(s_i)}(z) = H_0^{(s_i)} + H_1^{(s_i)} z^{-1} + H_2^{(s_i)} z^{-2} + \dots \tag{9}$$

$$H^{(s_i)}(z) = |H^{(s_i)}(z)| e^{j\phi_s(z)} = Gz^{-r} \underbrace{\prod_{i=1}^{L_1} (1 - \alpha_i z^{-1})}_{I(z^{-1}): \text{min. phase}} \underbrace{\prod_{i=1}^{L_2} (1 - b_i z)}_{O(z): \text{max. phase}}, \tag{10}$$

$i = 1, \dots, L$

where s_i stands for spatial location, and ϕ_{s_i} represents a non-random phase shift which is a function of frequency. The transfer functions of acoustic systems often exhibit wide dynamic ranges and very long impulse responses. The channel model describes the frequency response of the channel over a finite bandwidth. Moreover, the multichannel scenario obtains an increase of the mean signal power and consequently an increase of the SNR in the working environment. Since an MA model is assumed, the system can be described by its impulse response having the following generalized expression for the propagation path:

$$\hat{h}_n^T = [h_n^{(s_1)} h_n^{(s_2)} \dots h_n^{(s_L)}], h_n^{(s_i)} \in \mathbf{C}, \text{ or } \mathbf{R}$$

1) Ocean Acoustic Impulse Response (OAIR) Characterization

Underwater acoustic channels belong to the general class of fading multipath channels, where the multipath propagation causes time-spread of pulses arriving to receiver:

- 1) Variable multipath depends on the ocean depth and propagation path length. It causes frequency selectivity and spectral nulls in the amplitude characteristics of the transfer function.
- 2) Variable channel time variations depend on sea conditions: sea state, depth, wave spectra, internal waves.

Underwater acoustic channels are particularly difficult to model statistically due to the nonhomogeneous, nonstationary environment and the many acoustic noise sources. An analysis of tolerance to uncertainties in amplitude statistics for underwater channels produces designs requiring nonlinear detectors. The effects of the sound speed structure have a significant impact on the shape of the OAIR within the ducts and/or the low-intensity shadow zones where subtle features can be predicted. Propagation-induced distortions can be removed by deconvolving the data envelope from the model envelope, while knowledge of the sound speed dependent features enables deconvolutional schemes to restore useful signal parameters.

If more accurate models are desired, then the OAIR shallow water case would consist of a doubly spread surface channel $h_S(\tau)$, where the frequency spread is due to the random surface motion and the time spread due to the multipath structure, and a singly time spread bottom channel $h_B(\tau)$. The frequency and time spreads result in a received signal with broader bandwidth and of longer duration than the transmitted one respectively. The most accurate system model for the OAIR is a *nonlinear time-varying* filter impulse response. However, first-order approximation of OAIR would rely upon the linearity and superposition of the surface and bottom reflections so that linear time-varying models would be

sufficient
$$h(\tau, t) = \underbrace{h_{B_i}(\tau)}_{\text{Bottom channel}} + \underbrace{r(t)}_{\text{reverberation}} + \underbrace{h_{S_i}(\tau)}_{\text{Surface channel}} \mathcal{F}^* \rightarrow H(\omega, t).$$

Frequency spreading channel characteristics can be measured via bifrequency functions that indicate the amount of shifted energy from one frequency to another:

$$h(\tau, t) \xrightarrow{2-D \mathcal{F}^*} H_B(\omega_1, \omega_2). \text{ A further, model simplification is obtained by assuming a}$$

temporally and spatially invariant or range independent ocean, even though the OAIR depends on the source-receiver configuration geometry (the impact of the temporal changes to the impulse response is neglected).

Ray acoustics with lossy specular reflection from boundaries may be used for the channel model. It is assumed that the propagation takes place along several paths with significant signal strength, or alternatively that several normal modes have strong amplitude weighting:

$$h_n = \sum_{k=1}^N G_k \delta(n - k)$$

where G_k , k stand for transmission losses, and propagation delays respectively. They are independent of frequency, and independent of each other. The received signal is modeled as the sum of many scattered replicas of the transmitted sequence x_n , with spectra $X_n(\omega_0)$:

$$y_n = \sum_{k=1}^N G_k x_{n-k} \rightarrow Y_n = \sum_{k=1}^N G_k X_n e^{j\omega_0 n + \phi_k} \tag{11}$$

An averaged impulse response for the shallow water channel using a simplified 3-ray model for the shallow water case, can be formed by the contribution of a direct ray LOS, a reflected ray from the sea surface, and a bottom reflected ray. From the linear systems theory the output (i.e., the received sequence $y_n^{(s_i)} \in \mathcal{G}$), is given as the convolution of the transmitted data with the impulse response of the channel filter model:

$$y_n^{(s_i)} \in \mathcal{G} = x_n^c \in \mathcal{Q} + \underbrace{\frac{G_k}{\alpha_s^{(s_i)}} x_{n-k}^c}_{\text{surface reflection}} + \underbrace{\frac{G_l}{\alpha_B^{(s_i)}} x_{n-l}^c}_{\text{bottom reflection}} + n^{(s_i)}, \tag{12}$$

$$i = 1, \dots, M$$

where $n^{(s_i)} \in \mathcal{Q}$ represents the total AGN, at each individual sensor element, and includes ambient and flow noise, assuming to follow a Gaussian distribution (i.i.d.), wide-sense stationary and statistically independent from the transmitted data. The ambient noise has a non-zero space-time cross-correlation, with a low frequency concentration, while the flow noise is spatially uncorrelated from element to element. The OAIR contains information about environmental loss parameters, i.e. rate decay of reverberant tail, or the overall attenuation parameters $\alpha_s^{(s_i)}, \alpha_B^{(s_i)}$ (surface and bottom attenuation losses respectively), and k, l are the relative time delays between the direct and multipath components. The assumption of a time invariant channel OAIR implies a stationary random variable for the received sequence $y_n^{(s_i)} \in \mathcal{G}$. However, the ergodicity property is not valid directly for the unconditioned received data process $E\{y_n^2\}$, but only for the

conditioned random variable, i.e. the ensemble average $E\{y_n^2|h_k\}$ equals the temporal $\langle y_n^2 \rangle$. A non-Gaussian signal processing framework is assumed for the transmitted data distribution model. The initially transmitted white i.i.d. data $x_n^w \in \mathcal{Q}$ from the ACS's transmitter, acquires the colored properties due to reverberation effects. The sequence $x_n^c \in \mathcal{Q}$ is assumed to be a non-Gaussian if reverberation is present. Finally, $h_n^{(s)}$ are the unknown channel impulse response coefficients presented to the equalizer. They are obtained after sampling the resulting continuous impulse response representing the convolutional cumulative results of the transmit filter, the continuous time channel filter, and the receiver front-end noise rejection filter.

The transfer functions of acoustic systems often exhibit wide dynamic range and very long impulse response. Measurement of the OAIR with long reverberation is usually performed by using rectangular pulse as the source signal, therefore pulse width and amplitude are significant design parameters to be determined. For the case of underspread channels $B_D T_M < 1$, *instantaneous measurements* of the time spread channel are meaningful: $h_t(\tau) = \sum_{t=t_1}^{t_2} h(t, \tau) + n(t, \tau)$ where the observation interval is smaller than the channel time invariance interval, while with overspread i.e., $B_D T_M > 1$ any waveform becomes severely distorted by induced ISI and only *average-type measurements* can take place. The time spread factor T_M implies a coherent bandwidth $(\Delta f)_c$, which is the defined channel bandwidth in which either the amplitudes or phases of the two signals have a high correlation degree, and determines the so-called *channel frequency selectivity*. Frequency spreading and bandwidth broadening of received signal are determined by the Doppler spread factor B_D which implies a channel coherence time $(\Delta t)_c$ that determines whether it is *fast* or *slow fading*, and provides a measure of the time interval over which the transmitted symbols are relatively undisturbed by channel fluctuations.

2) Ideal Equalization Conditions

Dealing with ideal Nyquist pulses that satisfy the Nyquist criterion

$$\frac{1}{T} \sum_{m=-\infty}^{\infty} H\left(j\omega - jm \frac{2\pi}{T}\right) = 1 \tag{13}$$

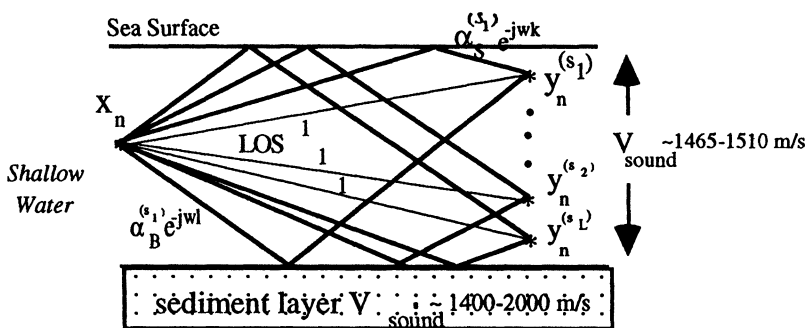


Figure 7 The 3-ray model in a shallow water multichannel scenario.

where $1/T$ is the Baud rate, then no ISI effects would appear. However, in practice we deal with bandlimited channels, so that high-level modulated data show severely degraded performance due to the ISI. This channel dispersion can be compensated with employment of equalization methods.

An equalizer decision rule $\delta_0^* \in \mathcal{A}$ is a rule or strategy for which the risk function $R(x, \delta) = k \text{ constant } \forall x$ data, or the loss function $L(\delta^*, \alpha) = k \text{ (constant } \forall \alpha \in \mathcal{A})$. Ideally, the channel and the equalizer transfer functions should be exactly inverse of each other in order to use the Zero-Forcing (ZF) optimization criteria [59] which force the intermediate samples of the equalized pulse to zero and the center sample to unity. Hence, the following constraint should be satisfied:

$$R(x, H, C) = \tilde{H}\tilde{C} = \tilde{I}z^{-d} = G[1 \mid 1]^T z^{-d}, G \in \mathbf{C}, d \in \mathbf{Z}^+, \tilde{C} \in \mathcal{A} \tag{14}$$

where $\tilde{C} = [C^{(s_1)} \mid C^{(s_2)}]$, $C^{(s_i)} \in \mathcal{A}$ is the coefficient vector of the combined equalizer (see fig. 8). The parameter G is a possible gain difference and z^{-d} is a linear phase shift producing a pure time delay d of the reconstructed sequence by half the time span of the equalizer. This delay is inconsequential in most cases. The equalizer reference tap is placed at the center, creating a noncausal structure, and is the only tap different from zero if the channel were the ideal Nyquist. An objective of all equalizers is a fast initial convergence, to achieve the smallest possible observation or training cost $C(n, s)$, and consequently to minimize the overall loss function $L(q, \alpha, n, s)$.

The channel covariance matrices $K_h^{(s_i)}$ would be positive definite matrices with a Toeplitz structure if the transfer functions $H^{(s_i)}(j\omega)$ were known not to present nulls on the unit circle, and if the sampling took place at the Baud rate respectively [35]. The elements of the $K_h^{(s_i)}$ are given by:

$$k_{ml}^{(s_i)} = \sum_j h_{(j-m)T}^{(s_i)} h_{(j-l)T}^{(s_i)} + \frac{E\{n_n^2\}}{E\{x_n^2\}} \delta_{ml}, \quad x_n, n_n \in \mathcal{Q} \tag{15}$$

where $E\{x_n^2\}$ and $E\{n_n^2\}$ symbolize the variance of the zero-mean value transmitted data, and the additive noise variance, respectively. Severely distorted channels present covariance matrices with larger eigenvalue spreads requiring a higher precision for the arithmetic representations.

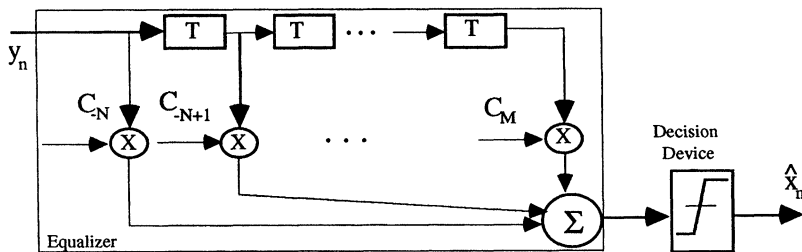


Figure 8 The tapped-delay line equalizer.

C. Second-Order Statistics (SOS) $\{S^{(2)}\}$, vs Higher-Order Statistics (HOS) $\{S^{(l>2)}\}$

If the OAIR can be estimated then, in principle, the inverse of the estimated response can be used to remove the distortion from the signal. In order to measure OAIRs, cross-correlation of the received signal with a source replica at the lower frequency band (and within a limited bandwidth), has been most often used. This process is equivalent to the propagation of the transmitted signal autocorrelation function R_x : $h_n = y_n * x_n = g_n * R_x + x_n * n$ (matched filter result). From (eq. 12), the autocorrelation of the received data $R_y(\tau)$, and the cross-correlation between the transmitted and received data $R_{xy}(\tau)$, are given by:

$$\begin{aligned}
 R_y(\tau) &= E\{y(t + \tau)y(t)\} \\
 &= R_x(\tau) + \alpha_S R_x(k + \tau) + \alpha_B R_x(l + \tau) + \\
 &\quad + \alpha_S R_x(\tau - k) + \alpha_S^2 R_x(\tau) + \alpha_S \alpha_B R_x(\tau - k + l) + \\
 &\quad + \alpha_B R_x(\tau - l) + \alpha_S \alpha_B R_x(\tau - l + k) + \alpha_B^2 R_x(\tau) + R_n(\tau) \\
 R_{xy}(\tau) &= E\{x(t + \tau)y(t)\} = R_x(\tau) + \alpha_S R_x(\tau + k) + \alpha_B R_x(\tau + l) \tag{16}
 \end{aligned}$$

Statistical independence between the transmitted data and the noise has been assumed, i.e., $x \perp n$. A higher-order statistical model description $\{S^{(l>2)}\}$ is assumed rather than one using only 2nd-order statistics $\{S^{(2)}\}$, and provides a better (closer to a full-order) statistical description $\{S^{(l)}\}$ by allowing independence assumptions on the statistics of the signal and noise data. By taking the Fourier transform of eqs. (16) the following spectral densities can be calculated:

$$R_y(\tau) \xrightarrow{\mathcal{F}} S_y(\omega), \quad R_{xy}(\tau) \xrightarrow{\mathcal{F}} S_{xy}(\omega) \tag{17}$$

It can be easily shown that the equalizer transfer function corresponding to a Best Linear Mean Square Error (BLMSE) [96] estimate that satisfies the orthogonality principle, i.e. $error\ e_n \perp data\ x_n$, should also satisfy the following condition (from eqs. (16) and (17)):

$$\begin{aligned}
 C^{(s_i)}(\omega) &= \frac{S_{xy}(\omega)}{S_y(\omega)} \\
 &= \frac{1 + \alpha_S e^{j\omega k} + \alpha_B e^{j\omega l}}{[1 + \alpha_S^2 + \alpha_B^2 + 2\alpha_S \cos(\omega k) + 2\alpha_B \cos(\omega l) + 2\alpha_S \alpha_B \cos[\omega(k - l)]] + S_n(\omega)} \\
 &= \{1 + \alpha_S^{(s_i)} e^{-j\omega k} + \alpha_B^{(s_i)} e^{-j\omega l} + \frac{P_n^{(s_i)}(\omega)/P_x(\omega)}{SNR(\omega)} (1 + \alpha_S^{(s_i)} e^{+j\omega k} + \alpha_B^{(s_i)} e^{+j\omega l})^{-1}\}^{-1} \tag{18}
 \end{aligned}$$

where $S_y(\omega)$ is the spectral density of the received signal, $S_{xy}(\omega)$ is the cross-spectral density of transmitted and received signals, and $P_n^{(s_i)}(\omega) / P_x(\omega)$ is the SNR which is

variable with frequency at each sensor element. For sufficiently large SNR level, the equalizer transfer function tends to the following limit:

$$C^{(s_i)}(\omega) \xrightarrow{SNR \gg 1} [1 + a_S^{(s_i)} e^{-j\omega k} + a_B^{(s_i)} e^{-j\omega l}]^{-1} \quad (19)$$

Then, for sufficiently small SNR $\ll 1$, the equalizer transfer function $C^{(s_i)}(\omega)$ weights differently the various portions of the band according to the corresponding SNR value at each frequency band. The Fourier domain transform of the receiver's reconstructed data \hat{x}_n is given by:

$$\hat{X}(\omega) = C(\omega)Y(\omega) + \underbrace{\frac{N(\omega)}{1 + \alpha_S e^{-j\omega k} + \alpha_B e^{-j\omega l}}}_{\text{Noise Term}}, C(\omega) \in \mathcal{A}, N(\omega) \in \mathcal{Q}, Y(\omega) \in \mathcal{G} \quad (20)$$

The inverse filter estimate $C^{(s_i)}(\omega)$, was derived based on *SOS* $\{S^{(2)}\}$ autocorrelation domain. However, *SOS* suppress the phase information which is significant in the recovery of non-minimum phase degraded systems.

More robust systems can be achieved via *HOS*-based estimators $\{S^{(l>2)}\}$, due to Gaussian noise suppression and phase information preservation (see section IV.A) [68]. An increase of the SNR level in the working environment is obtained, while the algorithm is capable of dealing with non-minimum phase channels. Higher order moments or cumulants or their Fourier Transforms, (so called polyspectra), can be used to identify and equalize distorted communication systems. More specifically it is the 4th-order (or higher) statistics domain that is most often used for communications applications, since communication signals have symmetric pdf, so that their 3rd-order statistics are identical to 0:

Third—Order Statistics (TOS)—domain: Skewness $\beta = E\{x_n^3\} = 0$

Fourth—Order Statistics (FOS)—domain: Kurtosis $\gamma_x = E\{x_n^4\} - 3\{E\{x_n^2\}\}^2 \neq 0 \quad (21)$

The 4th-order cumulant nonlinear functions of the received data can be used to provide channel phase estimates $\hat{\phi}_{(s_i)}$:

$$L_{m,n,l} = E\{y_i y_{i+m}^* y_{i+n} y_{i+l}^*\} - E\{y_i y_{i+l}^*\} E\{y_{i+m} y_{i+n}^*\} - E\{y_i y_{i+m}^*\} E\{y_{i+n} y_{i+l}^*\} \quad (22)$$

where the expected value $E\{*\}$ of the stochastic process due to the inherent environmental uncertainties is indicated, and its Z-transform, (the trispectrum) is as follows:

$L_{m,n,l} \xrightarrow{Z} T_{z_1, z_2, z_3}^y$. Note that the 2nd and 4th order moment estimates are updated iteratively with each new received symbol.

In addition to phase estimates $\hat{\phi}_{(s)}$, polyspectra techniques can detect and characterize nonlinearities of a system, and they have been applied in various areas [68] such as oceanography, geoscience, sonar and array signal processing, communications, biomedical engineering, speech processing, time series, etc.

D. Network Architecture Structure Issues

Applicability of blind equalizers has been investigated for frequency selective fading digital radio communication links. It has also been successfully applied in data communications, reverberation canceling, seismic deconvolution, and image restoration. Image restoration is applicable to underwater imaging systems with coherently illuminated submerged objects. There are also underwater acoustic communications scenarios where the blind equalizer may be used as part of the receiver.

From the standpoint of implementation, there are applications that are restricted from broadcasting any learning sequences \tilde{x}_n^{tr} towards the receiver by the system architectural concerns. In systems with network configurations such as centralized communication systems (where a base/master station exchanges messages with satellite/slave nodes), P-MP or MMDS networks, self-adjustment is not only desirable, but is required. An example case is found in an environmental monitoring application, where the self-adaptive scheme provides freedom to place the sensor at a variety of geographical locations $\{s_i\}$ without the wasted time and energy associated with sending long sequences of training data \tilde{x}_n^{tr} . In current schemes, the master or base station would receive training data \tilde{x}_n^{tr} from each sensor's location in order to identify each separate communication channel characteristics $h_n^{(s)}$. As a second example, we refer to a more critical application, where the base station transmits towards a group of receivers (i.e. provides control commands, or navigational/coordinational data to Autonomous Vehicles AUV's), but where one of the communication links $h_n^{(s)}$ fails. Under the conventional scheme the master control should interrupt the global data broadcast x_n , and intervene, initiating informationless training sequences \tilde{x}_n^{tr} . Under a blind scheme, the transmission to the remaining nodes is not interrupted while the failed node self-adjusts. In both examples, there is a necessity for the receiver's adaptive nature to keep track of the changing physical characteristics of the communications channel (source and receiver motion, and environmental fluctuations, e.g. temperature, salinity, etc.). The benefit from self-autoadjustment should be obvious (see Section VI).

4. MITIGATION STRATEGIES FOR INDUCED DISTORTIONS

The OAIR and the sidelobes strongly depend on the waveguide structure and the source and receiver positions. The motion and displacement from this position, as well as other environmental variabilities, impose a real-time adaptivity for the receiver operation to keep track of the fluctuations. Various self-adaptive communications techniques have been developed for digital radio scenarios [8], [12–14], [31], [37–38], [47], [67], [71–72], [85], and [90]. However, those techniques have not been designed for the singular characteristics of the oceanic environment. Furthermore, their performance is limited in terms of speed of convergence and robustness. OAIRs with long multipath spreads ($T_M \leq$

3sec) result in severe temporal signal dispersions. A deficiency of several compensation techniques used to equalize highly distorted underwater data communication links $h_n^{(s)}$, is the requirement that no constraints are put upon the correlation properties of the transmitted data $E\{x_n x_k\}$, causing inability to deal with reverberation effects and the colored correlation properties at the equalizer input $y_n^{(s)} \in \mathcal{G}$. Thus, improvements are needed in order to address the greater data rates $\in [100s\text{ KHz}, 1\text{ MHz}]$ and volumes required by video signal transmission. We are investigating a new algorithmic approach that includes the signal autocorrelation properties $E\{x_n^2\}$, in order to take into account the reverberation effect.

Equalization is of the most computationally-intensive DSP based functions of a communication system. There is clear need from an algorithmic and architectural respective. In particular, the class of HOS-based equalizers show various “cycle-hungry” algorithmic portions which support the need for computational optimization. Simplicity is among the top virtues in applications such as wireless personal communications services (PCS) and wireless underwater ACS. There is particular need for receiver hardware simplification in the development of compact, portable, low-power modems for applications such as wireless PCS, underwater ACS, etc.

To obviate the burden of equalization, an alternative compensation technique may be implemented using *MCM*. Since, the ocean waveguide shows resonance and optimal propagation over three basic modes, *MCM* may be used to reduce multipath effects and to increase the system margins against noise and ISI. A proposed new receiver configuration using *MCM* has low-complexity and provides low-power implementation.

A. Equalization in Digital Underwater Acoustics

1) Reverberant Environment

Acoustic reverberation varies in space and time and can be considered as a random time-varying linear function of the transmitted wave. A modified version of the *Multichannel Criterion with Memory Nonlinearity MCRIMNO* [12], can be applied, in order to minimize the variance of the multiple diversity receptions. The signal autocorrelation properties are also considered in order to take into account the reverberation effect.

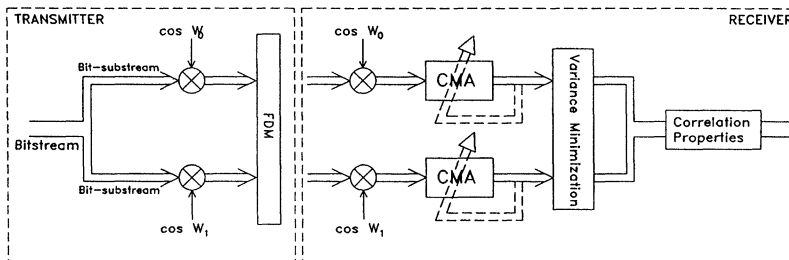


Figure 9 The parallel MCM transmission scheme.

The covariance of the reverberation or its intensity spectrum is, perhaps, the most important statistic. Accurate knowledge of the geometry of the configuration and the scattering mechanism enables prediction of the reverberation behavior. Otherwise, statistics are estimated from measurements and experimental data. Ensemble averages $E(\cdot)$ may be used with nonstationary data, as well as time-averages $\sum_n(\cdot)$, if stationarity and ergodicity assumptions apply on the data. Statistically large and valid data samples are necessary. Note that the stationarity assumption regarding the data, is more readily made for short length transmitted pulses $x_n^w \in \mathcal{Q}$. Let the reverberation covariance matrix be defined as $K_x(n, k) \stackrel{\Delta}{=} E\{x(n)x(k)\}$. For the case of covariance for a stationary reverberation: $K_x(n, k) = K_x(n - k)$. A more realistic case consists of the locally stationary model:

$$K_x(n, k) = \underbrace{\quad}_{\text{slowly}} \quad \underbrace{\quad}_{\text{stationary}} \cdot$$

varying covariance

In the two-sensor case, the two separate equalized outputs ideally at convergence should be identical within some finite relative time delay d . This condition is equivalent to the minimization of the MSE between the two individual equalizers' outputs $z_n^{(s)}$. There are two individual N-tap CRIMNO-based equalizers, combining their outputs with a MMSE criterion to minimize the output error signal variance. The adaptation is a gradient-type scheme minimizing the C-MCRIMNO cost function which includes memory *nonlinear* terms (z_n). The joint optimization criterion $U(r)$ is formed on the time, space and autocorrelation domain simultaneously in the space of performance measures \mathcal{M} :

$$U(r) = \underbrace{\sum_{j=1}^2 w_0^{(s_j)} E(|z_n^{(s_j)}|^2 - R_2)^2}_{\substack{\text{CMA part for} \\ \text{Equalizers 1 \& 2}}} + \underbrace{\sum_{j=1}^2 \sum_{i=1}^M w_i^{(s_j)} |E(z_n^{(s_j)} z_{n-c}^{(s_j)}) - K_x(i)|^2}_{\substack{\text{Correlation Part for} \\ \text{Equalizers 1 \& 2}}} + \underbrace{\sum_{k=0}^{M-1} w_{M+k+1} |e(n-k)|^2}_{\substack{\text{MMSE Part-Combination Term} \\ k = 0 \text{ Current Outputs Error} \\ k > 0 \text{ Past Outputs Error}}} \tag{23}$$

where $R_2 = E|x_n|^4 / E|x_n|^2$, $K_x(i) = E\{x_n x_{n-i}\}$ for $i = 1, \dots, M$ are the autocorrelation samples of the colored transmitted data distorted by reverberation, M is the memory length of the algorithm and equals the window length over the past outputs that contribute in forming the squared error function. In this case, $w_k^{(s)}$ are adaptive coefficients and can behave either as weights ("forgetting factors") to strengthen the algorithm's tracking capability, or that are bounded by thresholds to prevent ill-convergence of the algorithm:

the error $e(n) = z_n^{(s_1)} - z_n^{(s_2)} \in \mathcal{M}$ between the outputs of the multiple equalizers, the outputs $z_n^{(s_i)} = Y_n^{(s_i)T} C^{(s_i)}$ of the equalizers, the vectors of received data $Y_n^{(s_i)} \in \mathcal{G}$, and finally the tap-vectors $C^{(s_i)} = [c_1^{(s_i)} \dots c_N^{(s_i)}]$, $c_j^{(s_i)} \in \mathcal{A}$ of the individual equalizers are also. Due to the second additive term of the cost function equation, it is implied that *at the convergence point the equalized outputs $z_n^{(s_i)}$ of both sensors will satisfy the correlation properties of the transmitted data x_n* , while the third provides the equality among the diverse receptions.

2) Reverberation-free Environment

In the absence of reverberation (a case of white data), a criterion that combines constant modulus properties CMA based on the intuitive reasoning that the modulus of a QAM signal is a reasonable indicator of the degree of distortion present in the equalized signal (along with minimum variance [11]) is sufficient. In this case, there is no need for preservation of correlation (colored) properties of the transmitted data. The modified C-MCRIMNO algorithm could also be applied for the white-input case satisfying the independence property (or zero-correlation), but the modified MCMA is preferred being simpler in computational complexity. The M-MCMA is also faster and more robust algorithm in convergence compared to MCMA reported in [12]. Note that C-MCRIMNO and MCMA have been both designed to deal with multichannel scenarios with arbitrary impulse responses $h_n^{(s_i)}$, where common assumptions such as strong correlation of the relative delays $d^{(i)}$ of multiple paths and independence among frequency notches $\omega_0^{(i)}$, are not necessary.

B. Limitations—Open Research Problems

1. *Gaussian Statistics Limitation:* A communication system that transmits data sequences following Gaussian probability distribution function, is non-recoverable. If this is the case, then all the information is carried by the second-order statistics domain, since the higher-order are identically zero.

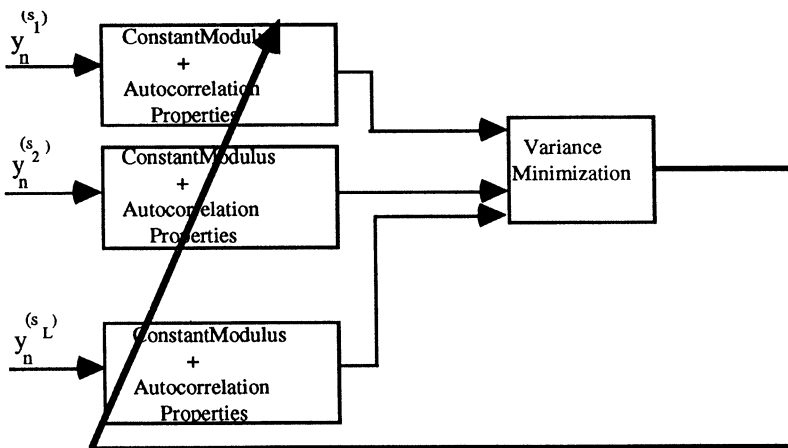


Figure 10 The modified M-MCMA linear blind adaptive equalizer structure.

2. *Local Minima Ill-Convergence:* Multimodal cost functions presenting local minima may prevent the system's global convergence. Existence of local minima in the single-sensor system's optimization cost function can render the system ill-conditioned and non-convergent (see Fig. 11). It has been well established that multichannel multisensor-based approaches can alleviate those limitations. Furthermore, the single-sensor deconvolution problem has been reported [8] as an ill-posed problem, imposing a requirement for multiple available measurements and multisensor-based equalization/deconvolution [12], [31], and [71] structures. In a different application (multiple target tracking in a cluttered environment) distributed sensors provide the desired total system observability [32–33], and [61].
3. *Unit Circle Transfer Function Limitation:* As the zeros of the channel's transfer function approach the unit circle, the linear equalizer's performance breaks down. Then, nonlinear structures as Decision Feedback (DFE) or MLSE are preferred. Moreover, the cepstrum-based methods [43], and references therein, are unable to deal with systems having zeros located exactly on the unit circle, since the cepstrum in these cases can not be determined due to its logarithmic type of definition [43].
4. *Effects of Finite-Length Equalizers:* It is well known that the more severe the distortion the higher the number of the necessary taps of the equalizer are required to obtain satisfactory equalization. From a system point of view, a severe distortion corresponds to channel models with zeros lying very close but not exactly on the unit circle (assuming MA channel models only). The positive definite property for the channel covariance matrix $K_h^{(s)}$ is preserved. Since the equalizer is the inverse filter of the propagation channel, it is implied that an Infinite Impulse Response (IIR) AR system would fully describe the equalizer filter's transfer function. It is the usual approach to approximate the inverse AR filter with an MA type. The success of the approximation increases with increasing order of the MA filter, and especially when the AR filter's poles approach the unit circle, i.e. the severe distortion case. Serious consideration should be taken regarding the selection of a *parsimonious order* for the equalizer length, since this is inversely proportional to the adaptation convergence speed. An arbitrary increase of the equalizer length causes undesirable increases of both the algorithm complexity and the time required for convergence.
5. *Phase ambiguity with the $k \pi/2$ -Phase Rotation Invariant class of Constellations:* For example, on transmitted QAM constellations (see Figure 5), phase rotations would not cause statistical changes in the channel output:

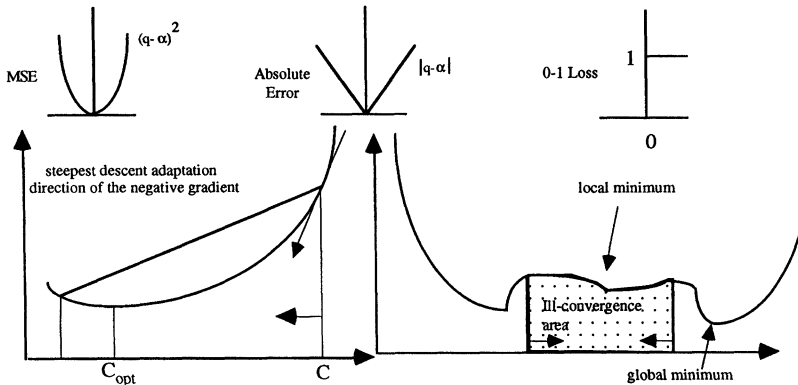


Figure 11 Various types of cost functions (top) Convexity for 1-D argument (bottom).

$$R(x,H,C) = \tilde{H}\tilde{C} = \tilde{I}z^{-d} = \frac{G'}{e^{j\omega k \frac{\pi}{2} G}} [1 \mid 1]^T z^{-d}, G',G \in \mathbf{C}, d \in \mathbf{Z}^+, \tilde{C} \in \mathcal{A} \tag{24}$$

Differential encoding could potentially solve the phase ambiguity problem.

C. Diversities

In some applications, including the underwater acoustics, the signal is received through various communication channels and the receiver has to jointly process all the received vectors, to minimize the P_e . This method, called *diversity reception* and it can be accomplished in time, frequency, space, angle, and electromagnetic field polarity. Then the received vector is given by:

$$\bar{Y}^T = [\bar{y}_1^T, \bar{y}_2^T, \dots, \bar{y}_M^T], \bar{y}_i \in \mathcal{G} \tag{25}$$

In addition to the potential for improving underwater network communications with adaptive equalization schemes, a proven record exists [7], [18], [25], [36], [73], [92], and [93] for spatial diversity methods in providing robust and reliable communications in multipath fading environments, i.e. tropospheric microwave digital and low frequency ionospheric radio. Wideband transmissions can be designed to exploit the diversity in the OAIR spread, and to make use of the multipaths rather than be constrained by their presence. Spatial diversity, which is optimum in terms of energy and temporal efficiency but not in the number of the deployed receivers, could exploit the inherent information redundancy of the surface reflected signal multidirectional scattering effects. Eventhough there is a need for the equalizer to reduce the increased ISI at higher bit-rates, use of spatial diversity can reduce the ISI and allow a simplified equalizer with lower complexity and implementational cost. That renders the system closer to a compact type unobtrusive portable unit. Moreover, use of diversity can pull the system to convergence when the adaptive equalizer operating alone can only drive the system to marginal functionality with inability to track the fast variations in the channel.

Frequency diversity may be implemented as an alternative for MCM methods for exploitation of the multiple modes of the ocean acoustic waveguide. The unique property of the oceanic waveguide with inherent multiple resonance modes can be exploited judiciously through a frequency diversity reception scheme, where the *source* employs Multiple Phase Shift Keying (MPSK) data modulation over both carriers: $X(\omega_1)$ and $X(\omega_2)$ are the transmitted spectra. The two carrier frequencies are the optimum propagational frequencies along the two ducts: ω_1 for duct-S (surface duct), and ω_2 (~ 50 Hz) for duct-D (deep sound channel) [51] (see fig. 12). Although improved performance can be obtained in terms of obtained SNR output levels, system degradation due to increased ISI effects is also expected. Equalization techniques using self-adaptivity are generally necessary in this case.

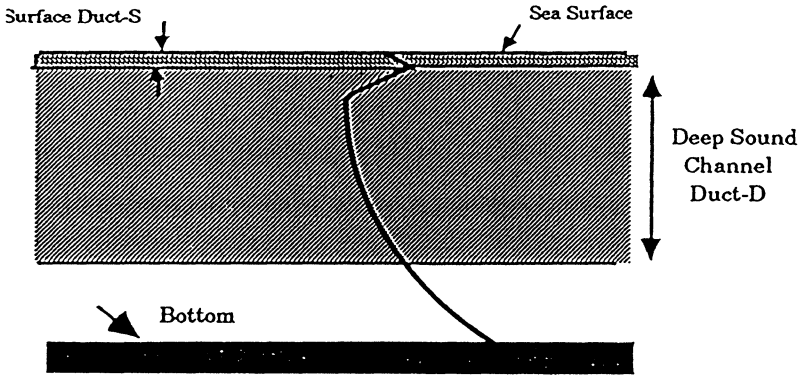


Figure 12 The multimodal acoustic ocean waveguide—Sound Speed profile.

D. Compound Strategies

In order to achieve the highest data rate transmission system, one can employ techniques that will combine self-adaptive equalization with embedded spatial diversity in the receiver's structure, or other forms of diversity receptions. The performance improvement can be evaluated in terms of convergence speed, data rate, SNR, Direct-to-Multipath Ratio (DMR), Signal-to-Reverberation Ratio (SRR), and BER ($\in \mathcal{M}$). It is also the MSE ($\in \mathcal{M}$) learning curve, whereby the Saltzberg bound [82] indicates a decreasing BER at lower MSE levels: $P_e < \frac{E\{z_n - x_n\}^2}{MSE}$.

1) Combination Self-Adaptive Equalization/Spatial Diversity

For low data rate applications, multipath reduction could consist of one or more of the following options: echo-canceling, beam steering, signal processing equalization, and signal correlation. In order to increase the reliability and the data rate of the system, there is need for employment of adaptive equalizers and diversity techniques by the receiver to augment its margins against noise, ISI, and equipment imperfections. In addition, use of auxiliary diversity can alleviate the receiver's hardware complexity resulting from equalization concerns. Using these techniques, the ocean channel can exhibit increased bandwidth margins W and should accommodate modulation schemes of higher spectral efficiency. The CTEA [43], C-MCRIMNO [11] techniques can function nearly optimally in both algorithmic and architectural sense under a MMDS acoustic system scenario.

In the following, we cite the "interfacing logic", i.e., the interdependence between the two different, but compatible disciplines, of channel equalization and diversity reception, to address the optimum sequence cofunctionality. The multiple separate equalized outputs $z_n^{(s_i)}$ at convergence should be identical within some finite relative time delay d . This condition is equivalent to the minimization of the multiple individual equalizers variance. We first consider $L > 2$ individual N-tap CRIMNO-based equalizers [11–12] combining

their outputs $z_n^{(s)}$ with the above criterion to minimize the variance of the output error signal $|e(n)|^2 \in \mathcal{M}$. By incorporating the above criterion in the cost function, a higher system margin is produced from the resulting lower BER in terms of both ISI and additive noise, and the statistical reduction in the overall distortion. The spatial coherence is controlled by monitoring the level of the cross-correlation function between the multiple measurements $y_n^{(s)} \in \mathcal{G}$, in terms of their distance s . The issue of non-correlated flow and ambient noise $\{n^{(s_i)}, i = 1, 2\}$ at the two sensors is critical depending on the inter-element separation s , so as not to increase the noise level by combining losses resulting from the receiver statistics through this additional processing, and is considered next.

Several techniques for effectively combining multiple received sequences can be formed in the space \mathcal{M} of performance measures; for instance, summing, weighted summing, or selection of the largest SNR channel. The MMSE technique (2-channel case) is more robust than the aforementioned three methods, when noise is present in one of the system channels. The less noisy channel will drive the other to convergence by playing the role of the desired reference training data. The diversity approach cancels the inherent positioning sensitivity of a single sensor and operates continuously on both signals $\{y_n^{(s_i)}, i = 1, 2\} \in \mathcal{G}$. *At convergence, the equalized outputs $\{z_n^{(s_i)}, i = 1, 2\}$ of both sensors will satisfy the correlation properties of the transmitted data x_n .* An increase of the obtained output SNR level can be immediately obtained, through a further processing of the resulting equalized outputs $z_n^{(s_i)}$ [11], [14].

2) Frequency/Spatial Diversity—Equalization

Introducing additional transmission redundancy will obtain robustness, channel error-resiliency, and reliability at higher rates. The proposed communication system employs a frequency diversity reception scheme consisting of two spatially diverse groups of hydrophones. The first vertical group of N hydrophones will occupy the depth of duct-S, while the second one with M ($M > N$) hydrophones will also extend vertically along most of the depth of duct-D, (see Figure 12). The method is expected to show robustness under environmental uncertainties regarding the statistical channel modeling and the mode amplitude statistics.

The receiver array is placed at a single depth and the broad bandwidth of the signal is utilized to equalize and/or identify the channel. Each of the ducts is equalized separately by the corresponding set of vertical spatial diversity equalizers and therefore intramodal distortions are compensated. The demodulated sets of sensor data for both arrays should be identical after equalization (except for a linear phase shift) leading to a minimization of the total variance of the $N + M$ multiple receptions $y_n^{(s_i)} \in \mathcal{G}$. Individual equalizers, based on constant modulus criterion, compensate for the induced ISI. The spatial diversity array with a minimum variance criterion, effectively reduces IMI among modes traveling along the same duct, caused mainly by the differences between the group velocities of the individual modes. Finally, the frequency diversity implementation provides an overall further system improvement and increases the output SNR.

Applying eigenanalysis of the wideband transmitted signal into its normal mode-components, the mode amplitude functions will be the eigenfunctions and the propagation constants will be the corresponding eigenvalues [51]. Proper array calibration by setting

the gain and the polarity of each hydrophone proportional to the amplitude of the desired mode, and using orthogonality of eigenfunctions of vertical pressure distributions can allow the arrays operate as mode filters [51] rejecting the interfering modes and noise. Then, depending on the environmentally imposed acoustic waveguide cutoff frequencies, equalization of the desired isolated single filtered propagating mode can be applied at each of the ducts. A highly absorbing bottom is assumed attenuating the higher-order modes propagating through the third bottom limited duct. The remaining modes that survive the absorption are rejected by the modal array filters.

5. UNDERWATER MULTIMEDIA SERVICE COMMUNICATION SYSTEM: DATA, STILL IMAGES, VIDEO

Deep Water Video Transmission

There are three primary applications for acoustic video telemetry, which impose complementary specifications, requirements and limitations:

1. *Inspection*: there is a need for high resolution good quality images, without the requirement for fast image updates or real time performance.
2. *Remote vehicle (ROV) piloting*: the image quality constraint can be relaxed, to provide an increased capability for fast image transmission in order to obtain full motion control of the vehicle.
3. *Biological Monitoring & Scientific Seafloor Survey*: high quality, color images and high speed images are usually required.

Compression techniques are significant in this application for reducing the required system bandwidth and the large data volumes for transmission. Differential pixel and frame coding are suitable techniques due to the poor lighting levels used with the underwater cameras causing an artificial similarity of neighboring pixels and stationary background. Compression types such as vector quantization, etc. are being investigated to obtain minimization of the signal processing delay and keep a high quality image. Most of the emphasis is given in the low frequency information recovery that has the strongest impact on the human perception. Image breakdown can be avoided via partially hiding the information loss through error-concealment techniques which are based on the redundant information that is inherent in the video signal [50]. Intraframe spatial as well as interframe temporal techniques are of interest in the high speed image (sequential) transmission for ROV piloting applications. In inspection applications where speed of transmission is not as critical as the image quality, sporadic frame losses are permitted without affecting human perception. For the intraframe techniques, damaged image blocks can exploit the reconstructed boundaries formed by the surrounding undamaged blocks [57]. There is a need to determine qualitatively sufficient schemes for the viewer, by combining compression coding techniques with the proper error correction and/or error concealment techniques. Interleaving techniques can be also used for correlated consecutive errors introduced by the fading channel.

All of the above techniques belong to the information-theoretic coding methods that exploit spatial and temporal correlation of the images-random signals in the spatial, temporal or transform domains. However, a different class of waveform coding which does not emanate from the information theory, consists the model-based coding whereby description based on the image structure can be obtained by taking into account 3-D properties inherent in the underwater scene. It has been reported [3] that very low transmission rates (down to 5 kbps) are obtained, and can be accommodated even by the strictly bandlimited underwater acoustic channel. A detailed study of typical underwater scenes can result in a structural-based classification in order to derive appropriate application-dependent model-based video coding.

In order to accomplish the stated goals under the most difficult of environmental conditions, it is possible to consider the possibility of using floating buoys with repeaters and regenerators, as well as through the use of array beamforming principles to guarantee LOS communications and obtain the required data rates. Under this configuration, the immunity to induced amplifier *nonlinearity* is given a higher priority in the modulation design procedure (see section II.D). Hence the class of constant-envelope modulations are suitable.

As an example of the potential for the proposed research and system implementational methods, Japanese researchers have recently reported [88] a technique for high-speed, reliable digital acoustic telemetry of color video between an underwater submersible at 3500 meters depth and a support-ship in a real-time fashion. The transmission was of 7 sec duration and consisted of a 256×256 pixel color image. In another approach [5], it was reported the transmission of images and data at a rate of 19.2 kbps on a 53 KHz carrier at distances of the order of 2000 m. The vertical link was used for this transmission by employing Phase-Shift Keying (PSK), and Frequency-Shift Keying (FSK) modulation at high baud rates.

6. APPLICATIONS

The need for improving the effectiveness of undersea ACSs is known and is recognized nationally and at the local level. Applications in the areas of offshore oil exploration and maintenance, environmental monitoring, ocean resources research, fisheries research, commercial fishing, construction, and aquaculture exist, as well as in other areas. Scientific research conducted in the oceans and coastal areas could benefit through the reduction of cost for acquisition and downloading of data from remote monitoring sites. Undersea robotics could benefit through improvement of the communications features of manned and unmanned underwater vehicles for control and for near real-time conveyance of data and images.

The proposed approach has particular potential for underwater vehicle operations as often required of AUV's, or Unmanned Underwater Vehicles (UUV's), where shallow-to-deep water, or short-to-long range excursions are typical. Degradation of acoustic data channels is well known to UUV and submersible operators, and can result in loss of vehicle contact, complicating navigation and control operations. Under these conditions, the system communications performance should adjust to the dynamically changing

environment, remain robust, and potentially reach the reliability of wired systems. Digital acoustic telemetry (acoustic modem) for real-time wireless transmission of time-critical sea data from instruments located in remote sections in the sea is of great significance for an undersea automated surveillance system, to transmit and receive data between submersibles, deep moored sensors and modems, and surface ships, land-based stations. That hydroacoustic link should be highly reliable at high speeds, and could be applied in the following application areas:

- Environmental monitoring
- Seafloor Survey: Real-time video transmission to the surface vessel displays is necessary for two reasons. First, in order to avoid lengthy recordings and data storage on the submersible's or the ROV's facilities which are limited. Second, the costs associated with diving time of a submersible would be exploited more efficiently if the scientific team on the surface vessel could watch on real-time the underwater operation and be able to assess the explored scenes, by communicating and interacting with the scientists in the submersible.

Fiber optics would be the ideal medium for data transmission, and is used in a variety of missions, including short range tactical and strategic military operations, however, it is cost-inefficient for those applications requiring repeated deployment or operation at great depths. Untethered ROV's [2], [16], [27–28], [54], and [79], based on wireless acoustic data transmission schemes might be considered ideal, in the sense of eliminating costly and sometimes unreliable umbilical cables, that conduct power and communications signals simultaneously. In general, little maintenance would be needed for an acoustic sensor communication system. To completely replace wired or optical communications links, ACSs will have to address the need for video transmission, particularly at depths exceeding 6000 meters where time delays inhibit real-time motion control. Image quality and transmission time require substantial improvement in reference to the current state-of-the-art in high speed acoustic data modem technology. Hence, the emphasis on enhanced acoustic transmission is highly desirable.

A further advantage of an all-acoustic data communications system is the potential of deploying multiply moored oceanographic sensors that would exchange and potentially pass data to a master station, forming a centralized-type communication network. Such systems which are characterized by geographical sensor deployment freedom, would have a positive impact on environmental monitoring efforts and might be crucial to certain scientific programs. The master unit might potentially be located at a great distance from the furthest slave unit in the monitoring chain if the acoustic link were reliable enough. Each unit would be required to *self-adapt* its communication parameters to the particular environmental conditions typical of its location—a task that is not readily achieved with present field-deployable system. Hence, the master station would not need to interrupt the global transmission towards each receiver in case of an individual unit link failure. Data could be recovered without disturbing the sensor mooring and without any wired connection.

Oceanographers, scientists, engineers, manufacturers, and managers collaborate to gain an understanding of the limitless unknowns of our marine environment. So there are

substantial needs for: Defense, offshore oil industry, environmental monitoring, ocean resources research, fisheries, and construction, public/tourist authorities, commercial fishing, tourist industry, research institutes, public environmental agencies, etc.

7. CONCLUSIONS—FUTURE WORK

We have reviewed the basic physical and theoretical limitations for communicating in an underwater acoustic environment. Advancement in underwater ACSs will involve new mathematical formulation and constraints (algorithm development) to implement more efficient, reliable, higher bandwidth acoustic systems for video and high data rate communications applications. The blind adaptation techniques proposed in this paper are capable of automatic node self-recovery in a P-MP network at the physical layer without the need for employment of higher level networking protocols. Implementation of correctional/recovery schemes at higher network levels than the physical layer necessarily reduce the communication system data throughput. This is due to the requirement for additional header information, and for more complex interaction between the different protocol layers during digital transmissions.

It is also worth considering the utilization of technology migration principles in using technical approaches similar to those employed in the wireless mobile terrestrial digital radio communications field. Eventhough the physics differ significantly, there are still enough similarities regarding the problem conditions so that under the proper modifications, already developed techniques could function in an underwater communications scenario. Analogies can be found in the following phenomena and techniques:

- Multipath propagation
- Frequency-selective fading
- Adaptive equalization/Diversity reception/Multicarrier Modulation
- Frequency reuse

Due to the intense high-frequency attenuations, the cellular concept of frequency reuse can be exploited as well, so that unique new network structures will be generated. Although one of the most critical factors in terrestrial cellular network design appears to be the performance using a large number of microcells, this is not necessarily the case in underwater ACSs design. However, it is still of great interest to establish what is the most critical among the aforementioned remedial strategies, and to which direction the research effort should be focused in the future.

Finally, a dynamic change of the system's transmission rate, depending on the current environmental conditions, to form a *multirate transmission* scheme, is another approach that has been adopted in wireless mobile radio networks to increase the system's average transmission rate [1], [106]. In an MCM transmission scheme, the rates on each carrier can vary providing a flexible transmission rate. Another advantage of the multirate transmission is that it provides modem flexibility and interfacing compatibility in terms of data rate, with existing terrestrial digital communication networks controlled by independent operating clocks.

Acknowledgments

This work was supported by the Harbor Branch Institute Postdoctoral program and, in part, by the Atlantic Foundation. This paper is HBOI contribution number 1114.

References

1. A.S. Acampora, and J.H. Winters, "A wireless network for wideband indoor communications", *IEEE J. Selected Areas Commun.*, Vol. 5, June 1987.
2. J. A. Adam, "Probing Beneath the Sea", *IEEE Spectrum Magazine*, April 1985.
3. K. Aizawa, and T.S. Huang, "Model-based Image Coding: Advanced Video Coding Techniques for Very Low Bit-Rate Applications", *Proc. IEEE*, vol. 78, no.4, April 1990.
4. M.M. Anderson, "Video Services on Copper", *Proc. IEEE ICC'91*, Denver, pp. 302–306, June 1991.
5. G. Ayela, M. Nicot, and X. Lurton, "New Innovative Multimodulation Acoustic Communication System", *IEEE, Proc. Oceans '94*, Vol. I, pp. 292–295, Brest, France Sept. 1994.
6. C.A. Belfiore and J.H. Park, "Decision Feedback Equalization", *Proc. IEEE*, Vol. 67, No. 8, pp. 1143–1156, Aug. 1979.
7. P.A. Bello, and B.D. Nelin, "Predetection Diversity Combining with Selectivity Fading Channels", *IRE Trans. Commun. Syst.*, vol. CS-10, pp. 32–42, March 1962.
8. C.A. Berenstein, and E.V. Patrick, "Exact deconvolution for multiple convolution operators-an overview, plus performance characterizations for imaging sensors", *Proc. IEEE*, vol. 78, no. 4, April 1990.
9. J.O. Berger, "Statistical Decision Theory and Bayesian Analysis", Springer-Verlag 1985.
10. A.G. Bessios and F.M. Caimi, "Reverberation Canceling for Data Communications in a Multimodal Acoustic Ocean Waveguide", *subm. IEEE Signal Processing/ATHOS Workshop, on Higher-Order Statistics, Spain 1995*.
11. A.G. Bessios, and F.M. Caimi, "Multipath Compensation for Underwater Acoustic Communications", *IEEE, Proc. Oceans 1994*.
12. A.G. Bessios, and C.L. Nikias, "Adaptive Blind Equalization with Multichannel CRIMNO Algorithm", *Digital Signal Processing*, no. 3, pp 16–28, Jan. 1993.
13. A.G. Bessios, and C.L. Nikias, "POTEA: The Power Cepstrum and Tricoherence Equalization Algorithm", to appear in *IEEE Trans. on Communications* Nov. 1995.
14. A.G. Bessios and N. Uzunoglu, "Self-Adaptive Equalizers with Space-Diversity versus Multipath Fading for High-Speed Microwave Digital Radio", accepted for publication in *Applied Signal Processing*, Springer-Verlag, 1995.
15. J.A.C. Bingham, "Multicarrier Modulation for Data Transmission: An idea whose time has come", *IEEE Communications Magazine*, pp. 5–14, May 1990.
16. P. Borot, D. Semac, and B. Leduc, "Acoustic Transmission of Pictures New Developments and Applications to Untethered Vehicles", *ROV 1985*.
17. P. Bragard, and G. Jourdain, "Adaptive Equalization for Underwater Data Transmission", *Proc. ICASSP 89*, pp. 1171–1174, Glasgow 1989.
18. D.G. Brennan, "Linear Diversity Combining Techniques", *Proc. IRE*, vol. 47, pp. 1075–1102, June 1959.
19. J.K. Chamberlain, F.M. Clayton, H. Sari, and E. Vandamme, "Receiver Techniques for Microwave Digital Radio", *IEEE Communications Magazine*, Vol. 24, No. 11, pp. 43–54, Nov. 1986.
20. C.S. Clay, "Optimum time domain signal transmission and source location in a waveguide", *J. Acoust. Soc. Am.*, vol. 81, pp. 660–664, March 1987.
21. C.S. Clay, "Use of arrays for acoustic transmission in a noisy ocean", *Rev. Geophys.* 4, pp. 475–507, 1966.
22. R. Coates, "Underwater Acoustic Communications", *Proc. Oceans '93*, pp. 420–425, Victoria Oct. 1993.
23. J.S. Collins, and J.L. Galloway, "Acoustic Telemetry of Video Information", *Proc. Oceans 1983*.
24. Colloquium on Signal Processing Arrays, IEE, London 1984.
25. B. Danielsson, and U. Johansson, "Measured improvements using angle and space diversity on a terrestrial microwave radio link", *Proc. Fourth European Conf. on Radio Relay Systems*, pp. 215–220, Oct. 1993.
26. L.B. Dozier, and F.D. Tappert, "Statistics of normal mode amplitudes in a random ocean. I. Theory", *J. Acoust. Soc. Am.*, vol. 63, pp. 353–364, Feb. 1978.
27. R.M. Dunbar et al., "Communications, Bandwidth Reduction and System Studies for a Tetherless Unmanned Submersible", *Proc. Oceans '81*, IEEE, New York, pp. 127–131.
28. R.M. Dunbar, A. Settery, D.R. Carmichael, and I. Anderson, "Cable-less Communications for Underwater Inspection, Engineering and Autonomous ROVs", *Underwater Systems Design*, Jan/Feb 1987.

29. R. M. Dunbar, "The role of tetherless ROVs in inspection", *International Underwater Systems Design*, Vol. 5, No. 1, pp. 9–15, 1983.
30. E. Feig, and A. Nadas, "Practical Aspects of DFT-Based Frequency Division Multiplexing for Data Transmission", *IEEE Trans. on Communications*, Vol. 38, No. 7, pp. 929–937, July 1990.
31. J. R. Fonollosa, J. A. R. Fonollosa, Z. Zvonar, and J. Vidal, "Blind Multiuser Identification and Detection in CDMA Systems", *IEEE, Proc. ICASSP—95*, Detroit, Michigan, 1995.
32. P. Forster, and F. Martinerie, "Passive Array Shape Calibration with Wide Band Sources of Unknown Location", *IEEE, Proc. Oceans '94*, Vol. I, pp. 235–240, Brest, France, Sept. 1994.
33. P. Forster, F. Ywanne, F. Martinerie, and D. Neveu, "New trends in sonobuoys array processing", *UDT 92*, London (classified session).
34. I.V. Gindler, Y.A. Kravtsov, and V.G. Petnikov, "Signal-to-noise ration in the reception of wideband pulses in dispersive media", *Soviet Physics Acoustics*, vol. 33, no. 3, pp. 260–261, 1987.
35. R.D. Gitlin, J.F. Hayes, and S.B. Weinstein, *Data Communications Principles*, Plenum Press, NY 1992.
36. M. Glauner, "Equivalence Relations between angle diversity and other diversity methods. Analytical model and practical results", *Proc. Fourth European Conf. on Radio Relay Systems*, pp. 261–266, Oct. 1993.
37. D.N. Godard, "Self-recovering equalization and carrier tracking in two-dimensional data communication systems", *IEEE Trans. Communications*, Vol. COM-28, No. 11, pp. 1867–1875, Nov. 1980.
38. F. Guglielmi, and C. Luschi, "Blind algorithms for joint clock recovery and baseband combining in digital radio", *Proc. Fourth European Conf. on Radio Relay Systems*, pp. 279–286, Oct. 1993.
39. S. Hara, M. Okada, and N. Morinaga, "Multicarrier Modulation Technique for Wireless Local Area Networks", *Proc. Fourth European Conf. on Radio Relay Systems*, pp. 33–37 Oct. 1993.
40. S. Hariharan, and A.P. Clark, "HF Channel Estimation Using a Fast Transversal Filter Algorithm", *IEEE Trans. ASSP*, Vol. 38, No. 5, pp. 1355–1362, Aug. 1990.
41. H. F. Harmuth, "Angular resolution of sensor arrays for signals with a bandwidth larger than zero", *IEEE Int. Symp. on Electromagnetic Compatibility*, pp. 316–320, 1980.
42. S. Haykin, "Adaptive Filter Theory", Prentice Hall 1989.
43. S. Haykin (ed.), "Blind Deconvolution", Prentice Hall 1992.
44. J.-P. Hermand, and I. Roderick, "Acoustic Model-Based Matched Filter Processing for Fading Time-Dispersive Ocean Channels: Theory and Experiment", *IEEE Trans. on Oceanic Engineering*, vol. 18, No. 4, Oct. 1993.
45. O.R. Hinton, G.S. Howe, and A.E. Adams, "An Adaptive, High-Bit Rate, Sub-Sea Communications System", *Proc. Europ. Conf. on Underwater Acoustics*, pp. 75–79, 1992.
46. "High-Speed Digital Subscriber Lines", *J. Selected Areas in Communications*, Vol. 9, No. 6, August 1991.
47. R. Iltis, J. Shynk, and K. Giridhar, "Bayesian Blind Equalization for Coded Waveforms", *Proc. MILCOM '92*, San Diego, CA Oct. 1992.
48. F. Ingenito, "Measurements of mode attenuation coefficients in shallow water", *J. Acoust. Soc. Am.*, vol. 53, pp. 858–863, 1973.
49. A. Jain, "Fundamentals of Digital Image Processing", Prentice Hall 1989.
50. F.C. Jeng, and S.H. Lee, "Concealment of Bit Error and Cell Loss in Inter-frame Coded Video Transmission", *IEEE Proc. ICC*, 1991.
51. F.B. Jensen, and W.A. Kuperman, "Optimum frequency of propagation in shallow water environments", *J. Acoust. Soc. Am.*, vol. 73, pp. 813–819, March 1983.
52. C.N. Judice, "Entertainment Video-on-Demand at T1 Transmission Speeds (1.5 Mbits/s), *Proc. SPIE Conf. on Visual Communications and Image Processing*, vol. 1001, pp. 396–397, Cambridge, Massachusetts, Nov. 1988.
53. I. Kalet, "The Multitone Channel", *IEEE Trans. on Communications*, Vol 37, No. 2, pp. 119–124, Feb. 1989.
54. K. Koskinen, P. Kohola, E. Murtoviita, J. Leppanen, and V. Typpi, "Hydroacoustic Transmission of Video Image for the control of a Remotely Operated Undersea Vehicle ROV", *Underwater Technology Symposium*, Tampere, Finland, 1990.
55. Y.A. Kravtsov, V.M. Kuz'kin, and V.G. Petnikov, "Resolvability of rays and modes in an ideal waveguide", *Soviet Physics Acoustics*, vol. 34, pp. 387–390, July–Aug. 1988.
56. B. Leduc, and G. Ayela, "Tiva a Self Contained Image/Data Acoustic Transmission System for Underwater Application", *1er Congres Francais d' Acoustique 1990*, Colloque de Physique, 51,2, Febr. 1990.
57. P.J. Lee, S.H. Lee and R. Ansari, "Cell Loss Detection and Recovery in Variable Rate Video", *Proc. Third Int. Workshop on Packet Video*, Morristown, New Jersey, March 1990.
58. N.S. Lin, and C-P. J. Tzeng, "Full-Duplex Data Over Local Loops", *IEEE Communications Magazine*, Vol. 26, No. 1, pp. 31–42, Feb. 1988.
59. R.W. Lucky, "Automatic Equalization for digital Communications", *Bell Syst. Tech. J.*, Vo. 44, pp. 547–588, April 1965.
60. A.A. Mal'tsev, and I.E. Pozumentov, "Adaptive spatial filtering of normal modes in an acoustic waveguide", *Soviet Physics Acoustics*, vol. 31, pp. 44–47, Jan.–Feb. 1985.

61. F. Martinerie, and P. Forster, "Data Association and Tracking from Distributed Sensors using Hidden Markov Models and Evidential Reasoning", IEEE, Proc. Oceans '92, Vol. I, Newport, Rhode Island, Oct. 1992.
62. K. Matsuda, Y. Nishizawa, and Fumio Amano, "Digital Signal Processing Technology for Communications", Fujitsu Sci. Tech. J., 28, 2, pp. 228–240, June 1992.
63. T.H. Meng, E.K. Tsern, A.C. Hung, S.S. Hemami, and B.M. Gordon, "Video Compression for Wireless Communications", Proc. Symposium on Wireless Personal Communications", pp. 14-1–14-17, Blacksburg, Virginia, 1993.
64. D.G. Messerschmitt, "Minimum MSE Equalization of Digital Fiber Optic System", IEEE Trans. on Communications, Vol. COM-16, pp. 1110–1118, July 1978.
65. D. Middleton, "Channel Modeling and threshold signal processing in underwater acoustics: an analytical overview", IEEE J. Ocean. Eng., vol. OE-12, no. 1, Jan. 1987.
66. D. Middleton, "Adaptive processing of underwater acoustic signals in non-Gaussian noise environments. I. Detection in the space-time threshold regime", Proc. NATO Advanced Study Institute, Adaptive Methods in Underwater Acoustics, pp. 527–535, 1985.
67. A. Neri, "Bayesian iterative method for blind deconvolution", Proc. SPIE '91, pp. 188–195, San Diego, CA July 1991.
68. C.L. Nikias, and M. R. Ranguveer, "Bispectrum Estimation: A Digital Signal Processing Framework", Proc. IEEE, Vol. 75, No. 7, July 1987.
69. A. Parvulescu, "Signal detection in a multipath medium by M.E.S.S. processing", *J. Acoust. Soc. Am.*, vol. 33, 1961.
70. F.G. Pedraja, and A del Pino, "Performance analysis of LMS adaptive filtering for PMP radio system applications", Proc. Fourth European Conf. on Radio Relay Systems, pp. 68–72, Oct. 1993.
71. A.P. Petropulu, "Identifiability of Blind Deconvolution of Non-white Signals", IEEE, Proc. Asilomar pp. 1245–1249, 1993.
72. G. Picchi and G. Prati, "Blind Equalization and Carrier Recovery Using a Stop-and-Go Decision-Directed Algorithm", IEEE Trans. on Communications, vol. COM-35, No. 9, pp. 877–887, Sept. 1987.
73. J.N. Pierce, and S. Stein, "Multiple Diversity with non-Independent Fading", Proc. IRE, vol. 48, pp. 89–104, Jan. 1960.
74. H.V. Poor, "Uncertainty tolerance in underwater acoustic signal processing", IEEE J. Ocean. Eng., vol. OE-12, no. 1, Jan. 1987.
75. M. Porter, and E.L. Reiss, "A numerical method for ocean-acoustic normal modes", *J. Acoust. Soc. Am.*, vol. 76, pp. 244–252, July 1984.
76. D.G. Powell, and A.G.J. Holt, "Novel Technique for time-delay beamforming", Electronics Letter, vol. 28, no. 2, pp. 190–2.
77. A.H. Quazi, and W.L. Konrad, "Underwater Acoustic Communications", *IEEE Communications Magazine*, pp. 24–30, March 1982.
78. S.U.H. Qureshi, "Adaptive Equalization", Proc. IEEE Vol. 73, No. 9, Sept. 1985.
79. V. Ranadive, "Video Resolution, Frame Rate and Grayscale Tradeoffs for Undersea Telemanipulator Control", MIT Man-Machine Systems Laboratory, March 1980.
80. W.D. Rummier, R.P. Coutts, and M. Liniger, "Multipath Fading Channel Models for Digital Microwave Radio", IEEE Communications Magazine, Vol. 24, No. 11, pp. 30–42, Nov. 1986.
81. B.R. Saltzberg, "Performance of an Efficient Parallel Data Transmission System", IEEE Trans. on Communications, Vol. COM-15, pp. 805–811, Dec. 1967.
82. B.R. Saltzberg, "Intersymbol Interference Error Bounds with Application to Ideal Bandlimited Signaling", IEEE Trans. Information Theory, Vol. IT-14, pp. 563–568, July 1968.
83. J. Salz, "Optimum Mean Square Decision Feedback Equalization", Bell System Tech. J., Vol. 53, No. 8, pp. 1341–1373, Oct. 1973.
84. G.H. Sandmark, and A. Solstad, "Simulations of an Adaptive Equalizer Applied to High-Speed Ocean Acoustic Data Transmission", *IEEE Trans. on Ocean Eng.*, vol. 16, no. 1, 1991.
85. Y. Sato, "A method for self-recovering equalization for multilevel amplitude-modulation systems", IEEE Trans. on Communications, vol. COM-23, pp. 679–682, June 1975.
86. E.H. Satorius, and J.D. Pack, "Application of Least-Squares Lattice Algorithms to Adaptive Equalization", IEEE Trans. on Communications, Vol. COM-29, pp. 136–142, Feb. 1981.
87. R.P.I. Scott, and P.J. Cooke, "Video Transmission using Millimetre Wave Radio Systems", Proc. Fourth European Conf. on Radio Relay Systems, pp. 311–315, Oct. 1993.
88. M. Suzuki, K. Nemoto, and T. Tsuchiya, "Digital Acoustic Telemetry of Color Video Information", Proc. 1989 International Symposium on Noise and Clutter Rejection in Radars and Imaging Sensors, IEICE 1989.
89. D.P. Taylor, and R.P. Hartmann, "Telecommunications by Microwave Digital Radio", IEEE Communications Magazine, Vol. 24, No. 8, pp. 11–16, Aug. 1986.
90. J.R. Treichler, and B.G. Agee, "A new approach to multipath correction of constant modulus signals", IEEE Trans. ASSP, Vol. ASSP-31, No. 2, pp. 459–471, April 1983.

91. J.M. Tribolet, "Seismic Applications of Homomorphic Signal Processing", Englewood Cliffs, NJ:Prentice Hall, 1979.
92. G.L. Turin, "On optimal diversity reception", IRE Trans. Inform. Theory, vol. IT-7, pp. 154–166, July 1961.
93. G.L. Turin, "On optimal diversity reception", IRE Trans. Commun. Syst., vol. CS-12, pp. 22–31, March 1962.
94. G. Ungerboeck, "Adaptive Maximum Likelihood Receiver for Carrier Modulated Data Transmission Systems", IEEE Trans. on Communications, Vol. COM-22, No. 5, pp. 624–636, May 1974.
95. R.J. Urick, *Principles of Underwater Sound*, McGraw-Hill 1983.
96. H.L. Van Trees, *Detection, Estimation and Modulation Theory*, John Wiley & Sons, NY 1968.
97. A.V. Vavilin, A.R. Kozel'skii, V.G. Petnikov, V.M. Reznikov, and E.A. Rivelis "Characteristics of the dispersion distortions of pulse signals in acoustic waveguides with absorption", *Soviet Physics Acoustics*, vol. 33, pp. 481–483, Sept.–Oct. 1987.
98. S. B. Weinstein, "A passband data-driven echo canceler for full-duplex transmission on two-wire circuits", IEEE Trans. on Communications, Vol. COM-26, No. 7, pp. 654–666, July 1977.
99. S. B. Weinstein, and P.M. Ebert, "Data Transmission by Frequency-Division Multiplexing Using the DFT", IEEE Trans. on Comm. Tech., Vol. COM-19, No. 5 Oct. 1971.
100. Q. Wen, and J.A. Ritcey, "Spatial Diversity Equalization for Underwater Acoustic Communications", *Proc. 26th Asilomar Conf.*, pp. 1132–1136, Pacific Grove, Ca 1992.
101. R.D. Widergren, "Motion Video at 56 kbps", Presentation at Teleconferencing Conference, Madison, Wiconsin, May 1983.
102. J.H. Winters, and R.D. Gitlin, "Electrical Signal Processing Techniques for Fiber Optic Communications Systems", IEEE Trans. on Communications, September 1990.
103. J.H. Winters, "Equalization in Coherent Lightwave Systems Using a Fractionally-Spaced Equalizer", *J. of Lightwave Technology*, Oct. 1990.
104. L. Wu, and A. Zielinski, "Multipath Rejection using Narrow Beam Acoustic Link", *Proc. Oceans '88*, pp 287–290, Baltimore Oct. 31–Nov. 2, 1988.
105. F. Xiong, "Modem Techniques in Satellite Communications", IEEE Communications Magazine, Vol. 32, No. 8, pp. 84–98, Aug. 1994.
106. K. Zhang, and K. Pahlavan, "An integrated voice/data system for mobile indoor radio networks", IEEE Trans. Vehicular Technology, Vol. 39, No. 1, pp. 75–82, Feb. 1990.

Special Issue on Time-Dependent Billiards

Call for Papers

This subject has been extensively studied in the past years for one-, two-, and three-dimensional space. Additionally, such dynamical systems can exhibit a very important and still unexplained phenomenon, called as the Fermi acceleration phenomenon. Basically, the phenomenon of Fermi acceleration (FA) is a process in which a classical particle can acquire unbounded energy from collisions with a heavy moving wall. This phenomenon was originally proposed by Enrico Fermi in 1949 as a possible explanation of the origin of the large energies of the cosmic particles. His original model was then modified and considered under different approaches and using many versions. Moreover, applications of FA have been of a large broad interest in many different fields of science including plasma physics, astrophysics, atomic physics, optics, and time-dependent billiard problems and they are useful for controlling chaos in Engineering and dynamical systems exhibiting chaos (both conservative and dissipative chaos).

We intend to publish in this special issue papers reporting research on time-dependent billiards. The topic includes both conservative and dissipative dynamics. Papers discussing dynamical properties, statistical and mathematical results, stability investigation of the phase space structure, the phenomenon of Fermi acceleration, conditions for having suppression of Fermi acceleration, and computational and numerical methods for exploring these structures and applications are welcome.

To be acceptable for publication in the special issue of Mathematical Problems in Engineering, papers must make significant, original, and correct contributions to one or more of the topics above mentioned. Mathematical papers regarding the topics above are also welcome.

Authors should follow the Mathematical Problems in Engineering manuscript format described at <http://www.hindawi.com/journals/mpe/>. Prospective authors should submit an electronic copy of their complete manuscript through the journal Manuscript Tracking System at <http://mts.hindawi.com/> according to the following timetable:

Manuscript Due	March 1, 2009
First Round of Reviews	June 1, 2009
Publication Date	September 1, 2009

Guest Editors

Edson Denis Leonel, Department of Statistics, Applied Mathematics and Computing, Institute of Geosciences and Exact Sciences, State University of São Paulo at Rio Claro, Avenida 24A, 1515 Bela Vista, 13506-700 Rio Claro, SP, Brazil; edleonel@rc.unesp.br

Alexander Loskutov, Physics Faculty, Moscow State University, Vorob'evy Gory, Moscow 119992, Russia; loskutov@chaos.phys.msu.ru